MICROVASCULARIZATION OF THE MIDBRAIN IN COMMON TREE SHREW (*Tupaia glis*)

CHURAIRAT DUANGCHAN

A THESIS SUBMITTED IN PARTIAL FULFILLMENT OF THE REQUIREMENTS FOR THE DEGREE OF MASTER OF SCIENCE (ANATOMY) FACULTY OF GRADUATE STUDIES MAHIDOL UNIVERSITY 2000

ISBN 974-664-139-5

Thesis
entitled

MICROVASCULARIZATION OF THE MIDBRAIN IN COMMON TREE SHREW (*Tupaia glis*)

Miss Churairat Duangchan
Candidate

Prof. Reon Somana,
M.D., Ph.D.
Major-advisor

Prof. Boonsirm Withyachumnarnkul,
M.D., Ph.D.
Co-advisor

Dr. Wisuit Pradidarcheep,
Ph.D.
Co-advisor

Prof. Liangchai Limlomwongse,
Ph.D.
Dean
Faculty of Graduate Studies

Assoc. Prof. Vijittra Leardkamolkarn,
Ph.D.
Chairman
Master of Science Programme
in Anatomy
Faculty of Science

Thesis
entitled

MICROVASCULARIZATION OF THE MIDBRAIN IN COMMON TREE SHREW (*Tupaia glis*)

was submitted to Faculty of Graduate Studies, Mahidol University

for the degree of Master of Science (Anatomy)

on

May 22, 2000

Churairat Duangchan

Miss Churairat Duangchan
Candidate

Reon Somana

Prof. Reon Somana,
M.D., Ph.D.
Chairman

Boon

Prof. Boonsirm Withyachumnarnkul,
M.D., Ph.D.
Member

Wisuit Pradidarcheep

Dr. Wisuit Pradidarcheep,
Ph.D.
Member

Sirinush Sricharoenvej

Asst. Prof. Sirinush Sricharoenvej,
Ph.D.
Member

Liangchai Limlomwongse

Prof. Liangchai Limlomwongse,
Ph.D.
Dean
Faculty of Graduate Studies
Mahidol University

Rassmidara Hoonsawat

Assoc. Prof. Rassmidara Hoonsawat,
Ph.D.
Acting Dean
Faculty of Science
Mahidol University

ACKNOWLEDGMENT

I would like to express my sincere gratitude and deep appreciation to my major-advisor, Prof. Dr. Reon Somana, for his kindness, guidance, supervision, suggestion, helpful criticisms and encouragement throughout the course of this training which have enabled me to carry out this study successfully. I am greatly indebted to Prof. Dr. Boonsirm Withyachumnarnkul, Dr. Wisuit Pradidarcheep, my co-advisors, for their valuable comments, suggestions and consultation. To Asst. Prof. Dr. Sirinush Sricharoenvej, my supervisory committee, Assoc. Prof. Wantanee Trakulrungsi and Assoc. Prof. Dr. Vijittra Leardkamolkarn, members of thesis proposal committee, for their valuable criticism, comments and suggestions. I would like to extend my gratefulness to Dr. Wichai Ekataksin from Department of Anatomy, School of Medicine, Tokyo Medical and Dental University, Japan for his valuable scientific advice and latest technical contributions to my study.

I wish to extend my sincere gratitude to Assoc. Prof. Ayudthya Samridthong, Dr. Somluk Asuvapongpatana, Mr. Sakporn Thongpila and Miss Sununta Chuncher for their advice and technical assistance. To Mr. Decha Boonranajitpilom, Mr. Koumkrit Pisetpaisan, Mr. Ittipon Phoungpetchara, Mr. Prasert Meeratana and all members of endocrine laboratory for their kindness and generous cooperation.

It is my great pleasure to thank Mr. Phon and Mrs. Vasana Phudphetkaew for their kindness and the financial support throughout the course of my study.

Finally, I wish to express my faith and deepest appreciation to all members of my family for their love, care, understand and endless support.

Churairat Duangchan

4136275 SCAN/M : MAJOR : ANATOMY ; M.Sc. (ANATOMY)
KEY WORDS : MIDBRAIN / COMMON TREE SHREW / MICROVASCULARIZATION

CHURAIRAT DUANGCHAN : MICROVASCULARIZATION OF THE MIDBRAIN IN COMMON TREE SHREW (*Tupaia glis*). THESIS ADVISORS : REON SOMANA, M.D., Ph.D., BOONSIRM WITHYACHUMNARNKUL, M.D., Ph.D., WISUIT PRADIDARCHEEP, Ph.D. 101 p. ISBN 974-664-139-5

The study of the midbrain in the common tree shrew (*Tupaia glis*) with vascular corrosion cast under a stereomicroscope and a scanning electron microscope (SEM) reveals that the midbrain is supplied by the branches of the vertebrobasilar system which are the basilar artery bifurcation, posterior cerebral, superior cerebellar, medial posterior choroidal and collicular arteries. They give off the penetrating arteries which radially course into the internal part of the midbrain and reach the cerebral aqueduct. This is the centripetal arrangement. The internal artery of the midbrain is divided into anteromedial, anterolateral, lateral and posterior groups according to the points of entry and territories that they supply. The penetrating arterioles terminate as capillary networks. The degree of capillary density in the midbrain is closely related the density of the nerve cells that accumulate in the areas of the midbrain nuclei. Less vascularity is obvious in the areas occupied by nerve fibers. The arterial anastomoses could be observed in the perimesencephalic or external part of the midbrain. The midbrain capillaries are without fenestrations. The venous drainage in the midbrain could be divided into three groups. The venous blood from the area ventral to the cerebral aqueduct drains into the tributaries of the veins of the anterior or petrosal group. The posterior group collects the venous blood from the collicular vein and the superficial vein of the quadrigeminal plate. The superior or galenic group receives the blood from the thalamocollicular, the lateral and dorsal aqueductal veins that empty the venous blood into the great cerebral vein of Galen, rectus sinus. Finally, the venous blood from both rectus and superior petrosal sinuses drain mainly into the external jugular vein and some into the internal jugular vein.

4136275 SCAN/M : สาขาวิชา : กายวิภาคศาสตร์ ; วท.ม. (กายวิภาคศาสตร์)

จุไรรัตน์ ดวงจันทร์ : การศึกษาโครงหลอดเลือดโดยละเอียดของสมองส่วนกลางในกระแต [MICROVASCULARIZATION OF THE MIDBRAIN IN COMMON TREE SHREW (*Tupaia glis*)]. คณะกรรมการควบคุมวิทยานิพนธ์ : เรือน สมณะ, พ.บ., Ph.D., บุญเสริม วิทยชำนาญกุล, พ.บ., Ph.D., วิสุทธิ์ ประดิษฐ์อาชีพ, ปร.ค. 101 หน้า. ISBN 974-664-139-5

การศึกษาโครงหลอดเลือดโดยละเอียดของสมองส่วนกลางในกระแต ด้วยเทคนิค vascular corrosion cast ภายใต้กล้องจุลทรรศน์และจุลทรรศน์อิเล็กตรอนแบบส่องกราด พบว่าสมองส่วนกลางได้รับเลือดจากแขนงของ vertebrobasilar system ซึ่งได้แก่ basilar artery bifurcation, posterior cerebral, superior cerebellar, medial posterior choroidal และ collicular arteries ซึ่งจะให้แขนงแทงทะลุเนื้อเยื่อของสมองส่วนกลาง ในแนวรัศมีพุ่งเข้าสู่ cerebral aqueduct หลอดเลือดที่เลี้ยงเนื้อเยื่อภายในของสมองส่วนกลางสามารถแบ่งออกเป็น 4 กลุ่ม โดยอาศัยจุดที่หลอดเลือดแตกแขนงเข้าสู่ภายในและขอบเขตที่ส่งแขนงไปเลี้ยง ซึ่งได้แก่ anteromedial, anterolateral, lateral และ posterior หลอดเลือดแดงเหล่านี้จะแตกแขนงเป็นหลอดเลือดแดงขนาดเล็กๆ และค่อยๆ ลดขนาดลง จนในที่สุดจะให้เป็นร่างแหของหลอดเลือดฝอย ซึ่งหนาแน่นในบริเวณที่เป็นกลุ่มของเซลล์ประสาทของสมองส่วนกลาง และมีความหนาแน่นน้อยในบริเวณที่เป็นเส้นใยประสาท ลักษณะของการเชื่อมติดต่อกันของหลอดเลือดแดงจะพบได้เฉพาะบริเวณผิวของสมองส่วนกลางเท่านั้น และพบว่าหลอดเลือดฝอยในสมองส่วนกลางเป็นชนิดไม่มีรูพรุนที่ผนังหลอดเลือด หลอดเลือดฝอยเหล่านี้จะรวบรวมเลือดดำเข้าสู่หลอดเลือดดำขนาดเล็ก เพื่อนำเลือดออกจากสมองส่วนกลาง ซึ่งแบ่งออกเป็น 3 กลุ่ม คือ บริเวณที่อยู่หน้าต่อ cerebral aqueduct ไหลกลับเข้าสู่หลอดเลือดดำในกลุ่ม anterior หรือ petrosal เลือดดำจากบริเวณ tectum จะไหลเข้าสู่ collicular vein และส่งเลือดดำต่อไปยัง rectus sinus ซึ่งเป็น posterior group กลุ่มสุดท้ายคือ กลุ่ม superior หรือ galenic รับเลือดจาก thalamocollicular, lateral และ posterior aqueductal veins ไหลเข้าสู่ great cerebral vein of Galen และส่งต่อไปยัง rectus sinus ในที่สุดเลือดดำจากทั้ง rectus sinus และจากกลุ่ม petrosal จะไหลเข้าสู่ transverse sinus เพื่อนำเลือดดำออกสู่ external jugular vein เป็นส่วนใหญ่และส่วนน้อยจะออกทาง internal jugular vein

LIST OF CONTENTS

LIST OF CONTENTS (CONT)

LIST OF FIGURES

Figure **Page**

LIST OF FIGURES (CONT)

LIST OF FIGURES (CONT)

LIST OF FIGURES (CONT)

LIST OF FIGURES (CONT)

LIST OF FIGURES (CONT)

LIST OF ABBREVIATIONS

a	=	arteriole
A	=	artery
ACA	=	anterior cerebral artery
ACoA	=	anterior communicating artery
AMV	=	anterior mesencephalic vein
BA	=	basilar artery
BV	=	basal vein
CA	=	cerebral aqueduct
CbC	=	cerebral cortex
Cbl	=	cerebellum
CC	=	crus cerebri
Cp	=	capillary plexus, capillary networks
CA	=	collicular artery
CG	=	central gray
CV	=	collicular vein
DSCP	=	decussation of superior cerebellar peduncles
EJV	=	external jugular vein
GVG	=	great cerebral vein of Galen
IC	=	inferior colliculus
ICA	=	internal carotid artery

LIST OF ABBREVIATIONS (CONT)

ICC	=	central nucleus of inferior colliculus
ICV	=	internal carotid vein
IF	=	interpeduncular fossa
IJV	=	internal jugular vein
Ip	=	interpeduncular nucleus
ISS	=	inferior sagittal sinus
LPChA	=	lateral posterior choroidal artery
LVCP	=	choroid plexus of lateral ventricle
Mb	=	mammillary body
MGB	=	medial geniculate body
MLF	=	medial longitudinal fasciculus
MPChA	=	medial posterior choroidal artery
N III	=	oculomotor nerve
Oc	=	oculomotor nuclear complex
OT	=	optic tract
P	=	pons
P1	=	first part of posterior cerebral artery
P2A	=	anterior half of second part of posterior cerebral artery
P2P	=	posterior half of second part of posterior cerebral artery
PCA	=	posterior cerebral artery
PCoA	=	posterior communicating artery

LIST OF ABBREVIATIONS (CONT)

PCoV	=	posterior communicating vein
Pi	=	pineal gland
PV	=	peduncular vein
R	=	red nucleus
RS	=	rectus or straight sinus
SC	=	superior colliculus
SN	=	substantia nigra
SPS	=	superior petrosal sinus
SS	=	sigmoid sinus
SSS	=	superior sagittal sinus
Tec	=	tectum
Teg	=	tegmentum
Th	=	thalamus
ThCV	=	thalamocollicular vein
Tr	=	trochlear nucleus
TS	=	transverse sinus
v	=	venule
V	=	vein
VA	=	vertebral artery
3VCP	=	choroid plexus of third ventricle

CHAPTER I

INTRODUCTION

The midbrain or mesencephalon is a part of brainstem situating between the diencephalon and pons. The caudal limit of the midbrain is represented by the decussation of superior cerebellar peduncles and trochlear nucleus, while the rostral part of the red nucleus, oculomotor nucleus and posterior commissure form the rostral limit (1). It consists of tectum, tegmentum and crus cerebri. The midbrain contains important nuclei, many ascending and descending fibers (2). Concerning the midbrain vascularity, it is nourished by branches from the circle of Willis. In submammals, the midbrain is supplied by only caudal division of internal carotid artery (3). In primitive and higher mammals, it receives the arterial blood from branches of the vertebrobasilar system, namely, basilar, posterior cerebral and superior cerebellar arteries (4). In human, the pattern of arterial supply in the internal portion of the midbrain could be divided into median and paramedian (antreomedial), anterolateral, lateral and posterior groups depending on their points of entry and areas that they supply (5, 6, 7). The midbrain blood supply has been reported in human (1, 5, 7), camel (8), cat (9), dog (10, 11, 12) and guinea pig (13, 14). It is quite similar among these species. The venous drainage is some what different and with minimal information.

So far, the knowledge concerning the midbrain vascularity has been focused on the main blood vessels. As the three-dimensional configuration of the midbrain vascular system is difficult to visualize by the histological study with light microscopy

(LM). The vascular corrosion cast technique using intravascular injection of casting medium in conjunction with scanning electron microscope (SEM) has been employed for detailed studies of the microangioarchitecture in various visceral organs in the field of anatomy (15). It is of interest to employ this technique to elucidate the midbrain microvascularization in common tree shrew (*Tupaia glis*), an animal regarded as a primitive primate (16, 17, 18, 19).

CHAPTER II

OBJECTIVES

As very little information concerning the detail vascularization of the midbrain has been reported, it is of interest to elucidate the gross anatomy, source of blood supply, ramification of the blood vessels within particular parts and microvascularization of the midbrain in commom tree shrew (*Tupaia glis*).

CHAPTER III

LITERATURE REVIEW

The midbrain consists of three major regions. They are tectum, tegmentum and crus cerebri. The tectum composes of four rounded prominences, the corpora quadrigemina. The upper two prominences are the superior colliculi or optic tectum in non-mammalians. The tectum is the laminated structure containing many layers of cells and fibers. The dendrites of many cells orientate in a radial fashion and the axons course in parallel to the surface. The colliculus lamination could be divided into superficial, intermediate (central) and periventricular zones (2). In human, the superior colliculus is subdivided into five strata. They are stratum zonale, stratum griseum, stratum opticum, stratum lemnisci and stratum profundum (20). The superior colliculus receives multiple inputs which terminate in the different zones and relating mainly to the head and eyes movements (2).

The two lower prominences are inferior or posterior colliculi or torus semicircularis in non-mammalians. It has three main divisions, namely, central nucleus, collicular cortex and peri-collicular tegmentum (21). The inferior colliculus is the site for the termination of auditory pathways, a center for correlation and control reflex in response to sound.

The second region of the midbrain called tegmentum situates ventrally to the tectum with the cerebral aqueduct being in between. It contains the rostral connection areas with the hindbrain, ascending and descending fibers, cranial nerve nuclei

(oculomotor, trochlear and mesencephalic trigeminal nuclei), red nucleus, interpeduncular nucleus, MLF and reticular formation. The midbrain tegmentum is the gateway for incoming and outgoing to and from the forebrain.

The third region is called crus cerebri. It is separated from the tegmentum by substantia nigra and made up principally of efferent fibers from the motor cortex, corticospinal and cortibulbar tracts (2). The right and left crus cerebri are separated by interpeduncular fossa (IF) (22). The substantia nigra (SN) is a layer of gray substance consisting of the melanin containing neurons and producing dopamine. It composes of zona compacta and zona reticulata being the important part of the extrapyramidal system (23).

Embryologically, the midbrain is derived from the mesencephalic vesicle during the fourth gestation week and undergoes less change than any other parts of the developing brain. The tectum is formed by the migration of the neuroblasts from alar plates. The neuroblasts from the basal plates give rise to groups of neurons in tegmentum. The substantia nigra may also be differentiated from the basal and alar plates. The crus cerebri becomes progressively more prominent as descending fiber groups pass through the developing midbrain (24). In addition, the embryonic development of the cerebral vascularization had been proposed by Kaplan (25). The constant relationship of the cerebral artery to the specific vesicles of the neural tube, the direction and position of arteries are governed by the anatomic location of the cellular masses (25). The arterial development of the midbrain is limited by branches of the vertebrobasilar system (26).

The arterial supply the human midbrain is very complex because it is significantly contributed by posterior cerebral artery (PCA) in addition to basilar artery (BA) and superior cerebellar artery (SCA) (1, 27). The rostral midbrain is supplied by branches of mesencephalic artery which is the distal division of BA. The branches of PCA and SCA nourish the caudal midbrain (25). The internal or penetrating artery of the midbrain has a relatively fixed pattern. The internal consistency was noted as early as 1873 by Duret (5) but lacking in the details of the exact point of entry, internal course and area of distribution. The internal arteries could be divided into several groups according to the points of entry and areas that they supply them (5, 6, 7). The internal or penetrating arteries could be concluded as following:

1. The paramedian group (anteromedial) is nourished by the perforating branches arising from the most distal BA that called mesencephalic artery (25), the proximal or P1-segment of PCA. (28, 29), the pars basalis (30), the basilar communicating artery (31) and the basilar bifurcation (32). The perforating arteries of this group are also branches of the initial portion of SCA (33). They run dorsally in the IF and penetrate near the midline (5). They are named median and paramedian branches (30), interpeduncular profunda (34), paramedian mesencephalic pedicle (35), paramedian peduncular artery (31, 36), posterior perforating of Gillilan (37) and mesencephalic perforating artery (29, 38). In addition, Percheron classified the paramedian artery as inferior paramedian mesencephalic artery (IPMA), superior paramedian mesencephalic artery (SPMA) and posterior thalamoperforating artery (PThA) (7, 33, 39). This group of arteries is well known

as "Paramedian thalamo-mesencephalic artery of Percheron" that commonly arises together as a single trunk and also supplies the thalamus (40).

2. The anterolateral group comprises the peduncular branches of collicular and accessory collicular arteries (28, 33, 41), posteromedial choroidal artery (PMChA) (7, 41), anterior choroidal artery (30), P-2 segment of PCA (42) and short circumferential artery (6). In addition, the arteries of this group may also arise from posterior communicating artery (PCoA), a lesser extent from SCA or even the BA (7). Branches of this group supply crus cerebri and adjacent parts of the midbrain (42) and the multiple small arteries terminate within the SN and supply lateral tegmentum (27).

3. The lateral group enters the midbrain from the lateral surface between crus cerebri and tectum in the ambient cistern (5). This group of artery is from branches of SCA, collicular artery and PMChA (7), ambient segment of SCA (43), short circumferential artery (6), lateral branch of collicular artery (44) and short circumferential from P-2 segment of PCA (1).

4. The posterior group consists of arteries that reach the quadrigeminal cistern and terminate or branch to penetrate the colliculus. They are long circumflex branch of PCA (28), quadrigeminal artery (5, 25), arteriae laminae tecti (45), accessory collicular artery of P-2 segment (7), quadrigeminal segment of SCA (43), tectal artery (25), collicular artery (41, 44, 46), medial superior cerebellar artery (7), posterior branch of SCA (47), and PMChA (7, 28). The branches of PCA supply superior colliculus, while those of SCA nourish inferior colliculus (28, 48). There are numerous anastomoses among branches of two arteries over the surface of colliculus (48, 49).

The blood supply of the midbrain of submammalian vertebrates (fishes, amphibians and birds) had been studied by gross dissection after injection with several media such as latex, gelatin, vinylite and Indian ink. It is shown that the arterial supply to the optic lobes is from only caudal branch of internal carotid artery (3). This is different from that of the primitive and higher mammals of which the blood supply to optic lobe is from the vertebrobasilar system (4). In camel, the anterior cerebellar artery and PCA give off mesencephalic branches to supply colliculi (8). In the dog and cat, the basilar bifurcation give off perforating branches supplying the medial zone of the midbrain while the tectal branches of the SCA join the tectal rami of PCA to form the collicular plexus (9). The arterial trunk of SCA gives off branches to supply crus cerebri and caudal colliculus but its distal branch supplies rostral colliculus (10). In addition, by injecting with Indian ink and 3% gelatin, the detailed vascularization in the dog mesencephalon includes tectum, tegmentum and crus cerebri, could be demonstrated (11, 12).

Recently, Majewska-Michalska (13) found that particular parts of the guinea pig midbrain is supplied by SCA, PCA, PCoA and choroid artery. In 1997, she focused on the angioarchitecture of the three parts of the midbrain by injecting with microfil silicone resin. The internal vessels divide into anterior, lateral and posterior groups according to the area supply. Among the three parts of the midbrain, the richest vascularization is observed in the tegmentum, which contains many nuclei. The degree of blood supply is proportional to the accumulation of nerve cells (14).

Although a lot of studies have been carried out in human and various animals, the report regarding to the midbrain venous drainage is very limited. By using a radio-

anatomical study in human, a separate drainage between tegmentum and crus cerebri had been demonstrated. The tegmental veins use the superior or Galenic's pathway but the vein of the base of midbrain have an anterior course draining inferiorly into superior petrosal sinus and/or superiorly into the basal vein (50). The venous blood from the tectum is drained into the specific channel calls "quadrigeminal vein". Such vein could be divided into superior and inferior quadrigeminal veins (51). In the dog and guinea pig, the veins are variable and shorter than the corresponding arteries (11, 12, 14).

As the three dimensional configuration of the midbrain vascular system is difficult to visualize by using light microscopic examination of the serial sections after injection with various substances. The vascular corrosion cast technique using the intravascular injection of methyl methacrylate has been introduced (52) and was successfully studied with scanning electron microscope (SEM) (53). This technique has been employed for detailed studies of microangioarchitecture in various visceral organs in the field of anatomy including the brains of human (54, 55, 56), rat (15), black bear (57, 58) and various organs of the common tree shrew including olfactory bulb (59), pituitary gland (60), pineal gland (61), cerebral cortex (62), cerebellum (63), hypothalamus (64), and choroid plexus (65). However, this technique has not been used to study microvascularization of the midbrain of any animal and human, except in anuran (66). It is of interest to employ this technique in conjunction with SEM to elucidate the midbrain microvascularization in the common tree shrews (*Tupaia glis*), an animal regarded as a primitive primate. (16, 17, 18, 19). Many authors had used tree shrews as a model for the study of visual function since the

animal is with a highly organized visual system (67). On the basis of the morphology of visual system and other criteria, this animal has been considered as the most primitive living primates (67, 68).

CHAPTER IV

MATERIALS AND METHODS

Animal Preparation

Fifteen adult common tree shrews (*Tupaia glis*) of both sexes weighing about 127.93 ± 4.92 g were divided into three groups. The first group was used for gross and morphological observation of the midbrain and relative structures under naked eyes and stereomicroscope. The second group was for histological study of the midbrain under light microscope (LM). The last group was for the study of blood supply and microvascularization of the midbrain with vascular corrosion cast technique in conjunction with stereomicroscope and scanning electron microscope (SEM).

Each animal was anaesthetized with diethylether. The thoracic cavity was opened to expose the heart, injected with 0.05 ml of heparin (Leo 5,000 iu/ml) into left ventricle and let it circulate for one minute. Then, a blunt needle was inserted into ascending aorta through left ventricle and clamped, the right atrium was cut to serve as the efferent port of the blood and injected fluid. Through this blunt needle, gentle perfusion with 200 to 250 ml of 0.9% NaCl solution was made to rinse the blood from the circulation until the efferent solution was clear.

Group I. Gross and Morphological Observation

Immediately after 0.9% NaCl perfusion, 200 ml of Bouin's solution was injected manually through the blunt needle to preserve the tissue. The head was removed and immersed in the same fixative overnight. Then, the head was corroded in

10 % formic acid for 2 to 3 days to remove the inorganic component of the cranial bone. The decalcification bone of the cranial halves was carefully removed to expose the whole brain. The cerebral hemisphere and cerebellum, then, were dissected to show the midbrain and relative structures and viewed with naked eyes, examined and photographed under stereomicroscope.

Group II. Routine Histological Preparation of the Midbrain

The fixative common tree shrew heads were rinsed several times in 70% alcohol until the yellowish solution was lighten. The skulls were decalcified in 10% formic acid for 2 to 3 days. The whole brain was removed, rinsed with tap water. The brains were sliced in sagittal and coronal planes at 2 to 3 mm thick with a sharp blade. Each sliced brain was dehydrated in a graded series of ethanol, cleared with xylene, infiltrated and embedded in paraffin. The embedded tissues were sectioned at 10 μm thick and stained with cresyl violet to evaluate the various areas of the midbrain. The stained sections were viewed and photographed under light microscope (LM).

Group III. Preparation for Studying the Midbrain Vasculature by Using Vascular Corrosion Casts Technique

After perfusing with 0.9% NaCl solution, the modified Batson's # 17 plastic mixture was prepared according to method described by Chunhabundit and Somana (69). Approximately 23 ml of plastic mixture was injected manually into ascending aorta via the same blunt needle at the rate of 8-10 ml/min (70). Most of the blood

vessels were completely filled with the plastic mixture as it was flowed out from the right atrium. The great vessels at the root of the heart were clamped to prevent the leakage of the plastic mixture. The animal was left at room temperature for 1 to 2 hours to let the plastic mixture hardening and complete polymerization of the plastic casts.

The heads of the common tree shrews were cut at the level of first cervical spine, removed skin and tissues and placed into 10% formic acid for 2 to 3 days to decalcify the bone. The brains were removed and divided into three groups. The cerebral hemispheres and cerebellum of the first group were removed to expose the brainstem. The second group was cross sectioned through the midbrain into three levels such as rostral, intermediate and caudal midbrain at 2 to 3 mm thick. The last group was cut into midsagittal and parasagittal sections at the same thickness. All of the three groups were placed in 40% KOH at room temperature for 5 days with daily changing of solution. Then, the corroded specimens were rinsed in tap water and gentle washed with distilled water to remove the remaining tissues. The vascular casts were frozen at -70°C and placed into the lyophilizer overnight. The dried vascular casts were examined under stereomicroscope to select the suitable areas for further investigation with SEM. The specimens were mounted on the metal stub, coated with gold/ palladium. The vascular casts were examined and photographed under SEM at accelerating voltage of 15 kV for study the microvascularization of the midbrain.

CHAPTER IV

RESULTS

In the common tree shrew, midbrain is the largest part of the brainstem. It is covered mostly by the occipital pole of the cerebral hemispheres and partially by the rostral portion of the cerebellum. It lies among the diencephalon anteriorly, cerebellum posteriorly and pons inferiorly (Figs. 1, 3). When cerebral hemisphere and cerebellum have been removed, the dorsal aspect of the midbrain is seen as a prominence with approximately 8 mm long, 5 mm wide and 6 mm high (Fig. 1). The superior colliculus is ovoid and relatively large while the inferior colliculus appears as a small strip situating under the caudal end of superior colliculus (Figs. 1, 3). The small portion of the crus cerebri is seen from the ventral aspect of the brainstem (Fig. 2). There is a furrow between the two crura cerebri and the oculomotor nerves emerge through it. The upper border of the midbrain is limited inferiorly by the optic tract and the mammillary bodies. Its lower end is marked by the pontomesencephalic sulcus.

The LM studies of the coronal sections stained with cresyl violet reveal that the midbrain nuclei are dark and the fibers are relatively lighter. The internal structure of the midbrain could be divided into three important regions as tectum, tegmentum and crus cerebri (Fig. 4). The tectum composes of superior and inferior colliculi which are the mounds of gray matter. The superior colliculus could be divided into superficial, intermediate (central) and periventricular gray zones. It is seen as

laminated structure with six strata due to the arrangement of nerve cells and fibers. As seen in Figure 5, the superficial zone is subdivided into stratum zonale (SZ), stratum griseum superficiale (SGS) and stratum opticum (SO). The intermediate zone consists of stratum griseum intermediale (SGI) and stratum album intermediale (SAI), while the deep or periventricular zone comprises only the stratum griseum profundum (SGP) that adjacent to the central gray. Within the various tectal layers, multipolar cells are present. The optic fibers are seen as a small band entering the ventrolateral side of the superior colliculus (Fig. 5). The inferior colliculus consists of the pericentral, external and the central nucleus of small sized-multipolar cells surrounded by a capsule of white fibers from lateral lemniscus (Fig. 6).

The tegmentum situates ventrally to the cerebral aqueduct containing gray columns and tracts. It situates between the pons and thalamus. The major groups of neurons in the tegmentum are oculomotor nuclear complex, nucleus of trochlear nerve, Edinger-Westphal nucleus, interpeduncular nucleus, mesencephalic nucleus of trigeminal nerve and red nucleus. In the cross section, the oculomotor nuclear complex appears as the interval between V-shape of MLF (Fig. 8). It lies rostrally to nucleus of trochlear nerve and extends to the rostral part of the superior colliculus. The fascicles of the oculomotor nerve course ventrally through the medial side of red nucleus and emerge from the medial part of the crus cerebri and lateral to interpeduncular nucleus. The nucleus of trochlear nerve is seen at the transitional level of the superior and inferior colliculus (Fig. 9). It situates caudally to the oculomotor nucleus and indents the dorsal surface of the MLF. The Edinger-Westphal nucleus is a small collection of neurons seen in the plane of rostral midbrain. It lies close to the

midline and dorsal to the ventral part of oculomotor nucleus at the diencephalon-mesencephalon junction. The mesencephalic nucleus of trigeminal nerve is a scattered strand of small neurons seen in the lateral part of central gray (Fig. 8). The interpeduncular nucleus is a group of cells lying between the two crura cerebri. The red nucleus is a large group of neurons occupying the major part of the tegmentum (Fig. 7). It is a round rod of gray matter and extends from the subthalamic regions at the level of mammillary bodies to the caudal end of superior colliculus which is marked by the decussation of superior cerebellar preduncles. The red nucleus could be divided into pars magnocellularis and pars parvicellularis. The important fiber tracts that could be observed in the tegmentum are MLF, medial lemniscus, lateral lemniscus and decussation of superior cerebellar peduncles.

The substantia nigra (SN) is a curve plate of gray matter situating between the tegmentum and crus cerebri (Fig. 7). It could be subdivided into pars compacta, pars reticulata and pars lateralis. The last part of the midbrain is the crus cerebri that is a small band of white matter under SN. It contains many descending fibers of motor tract from the cerebral cortex (Fig. 4).

The study with vascular corrosion cast technique reveals that the arterial supply of the common tree shrew brain is from internal carotid and vertebrobasilar systems (Fig. 10). Two vertebral arteries (VA) join one another to form a single basilar artery (BA) at the level of the pontomedullary junction. The BA ascends on the ventral surface of pons in the midline and divides into superior cerebellar (SCA) and posterior cerebral (PCA) arteries at the pontomesencephalic sulcus. The internal carotid artery (ICA) gives off anterior cerebral (ACA) and middle cerebral (MCA)

arteries. The anterior communicating artery (ACoA) connects between two ACA. Moreover, the posterior communicating artery (PCoA) communicates between PCA and ICA. Thus, the complete arterial circle of Willis at the base of the brain in the tree shrew is evident (Fig. 10). It is obvious that the blood supply of the midbrain in common tree shrew is from the branches of the vertebrobasilar system, namely the BA, SCA and PCA (Fig. 13). However, the branches from the PCA are the major sources (Figs. 15, 16). The PCA has three types of branches as cortical, central and ventricular branches. The cortical branches mainly supply the cerebral cortex. The central branches convey the blood to the midbrain and other parts of the brainstem. The ventricular branches become the choroid plexuses of the third and lateral ventricles and extend some branches to supply the midbrain. After branching from BA, the PCA could be divided into P_1 to P_4 segments. The P_1 segment is proximal to the stem of the PCoA. It gives off direct perforating branches and peduncular branches to supply the ventromedial and ventrolateral parts of the midbrain. The P_2 segment extends from PCoA in the ambient cistern. It subdivides into anterior (P_2A) and posterior (P_2P) halves (Fig. 17). The P_2A is next to PCoA and runs in parallel to basal vein (BV). It gives off the lateral posterior choroidal artery (LPChA) that enters the choroid plexus of lateral ventricles and also supplies the metathalamus. The P_2A also sends branches to supply the cerebral cortex. The P_2P courses in parallel to the P_2A, inferior to BV and inferolateral to medial geniculate body (MGB). It could be subdivided into collicular and medial posterior choroidal (MPChA) arteries at the inferior pole the MGB (Fig. 17). The collicular artery gives off three to four branches distributing in tree-like pattern to reach the quadrigeminal plate of the midbrain

(Fig. 18). The MPChA extends from P2P and encircles the midbrain at the junction between upper end of superior colliculus and lower part of the thalamus. It sends branches to supply the superior colliculus and the choroid plexus of third and lateral ventricles. The MPChA and collicular arteries in the quadrigeminal cistern seem to be the P3 segment and the terminal branches to the cerebral cortex are the P4 segment. The superior cerebellar artery (SCA) is a branch of BA that emerges under the origin of PCA (Figs. 14, 17). It is separated from the PCA by the third cranial nerve. It then runs in parallel to the vein of the pontomesencephalic sulcus. The SCA is the main branch supplying the pons and the cerebellum. It also sends collicular branch to nourish the caudal pole of the inferior colliculus. The BA also gives off perforating branches at the basilar bifurcation to supply the midline portion of the midbrain and thalamus through the interpeduncular fossa (IF).

As seen in the cross sections of the vascular corrosion cast, the internal part of the midbrain receives the blood from the penetrating branches of the parent arteries that encircle the midbrain (Figs. 13-18). These penetrating branches run in the radial pattern towards the cerebral aqueduct (Fig. 11). According to their points of entry and areas of distribution, these internal radial branches could be divided into anteromedial, anterolateral, lateral and posterior groups. In the anteromedial group, the paramedian arteries are the longest vessels but less in number (Fig. 12). They are usually four. The posterior group is the highest in number of penetrating vessels when compares among the three parts. It is noted that the characteristics of these penetrating branches are the centripetal direction.

The study of the midsagittal sections of the midbrain illustrates the paramedian branches as the direct perforating branches from the basilar bifurcation, SCA and from the P1 segment of PCA (Fig. 12). They enter the midbrain in the fan-like manner to supply the medial part of the midbrain. The paramedian thalamomesencephalic artery is the branch of basilar bifurcation or the P1 segment of PCA. It supplies the midbrain and the thalamus. The paramedian arteries distribute in the areas of interpeduncular fossa (IF), crus cerebri and tegmentum. Finally, they end at the ventral part of the cerebral aqueduct. The tectum which is the area dorsal to the cerebral aqueduct does not receive the blood from arteries of this group but they are from the posterior group.

In order to visualize the distribution of the blood vessels in the various areas of the midbrain, the cross sections of vascular corrosion cast are performed at rostral, intermediate and caudal ends of the midbrain (Figs. 20, 22, 24). The histological sections of the similar levels to the sections of the vascular corrosion cast are put for comparison (Figs. 19, 21, 23). Among the three parts of the midbrain, the tegmentum is the most vascularized area as it contains many nuclei or groups of neurons. The arteries of the anteromedial group that supply the area of the tegmentum are the branches of the basilar bifurcation, SCA and of the initial portion of PCA. They give off direct perforating branches to supply the medial portion of the midbrain (Fig. 22). The oculomotor nuclear complex is supplied by the paramedian thalamomesencephalic branches (Figs. 22, 25 ,26). The right and left paramedian branches run in the IF and penetrate the midbrain at right angle near the midline. They run in parallel to each other in the dorsal direction to reach the floor of the

cerebral aqueduct and also run in curves, arcuate and pass laterally before entering the oculomotor nerve nuclear complex. They embrace the area corresponding to the medial side of the red nucleus and also supply nucleus of trochlear nerve, MLF and decussation of superior cerebellar peduncles. The collateral circulation among the arteriolar branches of the right and left paramedian arteries have not been observed. The anterolateral group consists of the penetrating branches of P1 and SCA (Fig. 25). The peduncular branches of P1 segment supply the crus cerebri and some of them pass through the crus cerebri to supply the SN, lateral side of red nucleus and of CN III and CN IV nuclei. It is noted that the arteries of this group do not reach the cerebral aqueduct. The lateral group is the penetrating branches of the initial portion of the collicular and MPChA arteries that supply the lateral part of the crus cerebri, lateral lemniscus and lateral part of the tegmentum. The branches forming the posterior group come from the collicular artery of P2P, SCA and MPChA. They give off branches to penetrate the colliculus (tectum). Many small arteries are seen to pierce the surface of the colliculus and end at various levels that relate to the arrangement of the layers of superior colliculus (Fig. 25). The dense vascularization is seen in the stratum griseum superficialis, stratum griseum intermedialis and central gray. At the level of inferior colliculus, the vascular density in the central nucleus of inferior colliculus is much higher than that in the superior colliculus.

When examining the midbrain vascular corrosion cast in the cross section at higher magnification (Figs. 27, 28), it is seen that the penetrating arteries give off arterioles and capillary beds inside the midbrain. The dark area indicates the high density of the capillary networks. The high density of the capillaries correspond to the

midbrain nuclei in the tectum and tegmentum. They are superior colliculus, inferior colliculus, oculomotor nuclear complex, trochlear nucleus, interpeduncular nucleus, interstitial nucleus of MLF, red nucleus and SN. It is noted that within the SN, the pars compacta has the most vascular density. The scantly capillary plexuses are usually found in the areas which contain nerve fibers. They are the areas of the crus cerebri, decussation of superior cerebellar peduncles, medial and lateral lemniscus. It is evident that medial part of the crus cerebri has the richest blood supply in comparison with lateral and central part.

When observing the vascular corrosion cast under SEM, it could also reveal that the common tree shrew midbrain receives the arterial supply from many sources (Fig. 29). They are BA, SCA and PCA (Fig. 29). The basilar artery bifurcation gives off the perforating branches to supply the midline region through IF. The PCA gives off some peduncular branches which anastomose on the outer surface of the crus cerebri. In the lateral aspect of the midbrain, the branches of P2A and P2P are shown (Fig. 30). The dorsal surface of the midbrain (quadrigeminal plate) is supplied by the collicular branches of P2P (Figs. 31, 35). There are a lot of arterial anastomoses on this collicular surface. The initial course of small arteries is in parallel to the collicular surface. They penetrate perpendicularly into the internal part the colliculus (Figs 32, 33). The small arteries usually cross over the superficial collicular veins.

After originating from the parent arteries on the surface of the midbrain, the arterial branches could be divided into two sets of the penetrating arteries. The superficial set breaks into arterioles and capillary networks in the superficial layer of the superior colliculus. The set of longer arteries goes deeper and ramifies into

capillary networks in the deep and central gray layers. It is evident that three microvascularization layers could be observed (Fig. 31). The superficial layer is the densest capillary networks. The vascular connections among branches of the penetrating arteries have not been observed. It is noted that the arterial sphincter are often seen at the branching site of small artery (Figs. 41, 42). After branching from the parent artery at the surface of the midbrain, the penetrating arteries rapidly reduce in diameter (Figs. 41). Occasionally, the smooth muscle cells are seen wrapping around the arteries (Fig.43). It is obvious that the capillary networks in the areas of midbrain nuclei are higher density than in the areas of nerve fibers when examine under SEM (Figs. 39, 40). When the surface of capillary casts is observed at high magnification, it appears very smooth indicating that the capillaries in the midbrain is without fenestrations (Fig. 45).

The venous blood from the capillary networks is collected into small venules (Figs. 44) and further into the tributaries of veins before being emptied into the larger veins at the surface of the midbrain. The capillaries in the central part of the midbrain around the central gray and the oculomotor nuclear complex collect the venous blood upward and dorsally into the lateral and dorsal aqueductal vein (Figs. 25, 26, 38). This joins with the thalamocollicular vein that lies in the edge between the superior colliculus and the thalamus (Figs. 18, 34). In some cases, lateral and dorsal aqueductal veins connect directly to the great vein of Galen. The venous blood from the tegmentum and crus cerebri (ventral part to cerebral aqueduct) are drained into the collecting veins which have the larger diameter than that of the accompanying arteries (Fig. 34). These collecting veins empty the blood into the posterior communicating

vein that lies in transverse direction in the IF and connects between the peduncular vein and BV (Figs. 36, 37). Some small veins drain the blood into the vein of pontomesencephalic sulcus that situates between the pons and the crus cerebri. The BV and vein of pontomesencephalic sulcus end at the junction between the superior petrosal sinus and transverse sinus (Fig. 24). The thalamocollicular vein originates from the BV which connects to superior petrosal sinus via lateral mesencephalic vein and then encircles the midbrain beneath the MPChA at the junction between the superior colliculus and the thalamus (Figs. 18, 34). It receives the venous blood from the both areas and drains into the great cerebral vein of Galen and rectus sinus, respectively. Some small veins at the dorsal surface of the caudal part of superior colliculus drain the venous blood directly into transverse sinus. At the junction between the superior and inferior colliculi there are two small veins running from each side and join one another at the midline before draining the blood into the dorsal aqueductal vein. After joining, it runs upward along the midline and connects with two or three veins of the colliculus at the caudal end of the quadrigeminal plate to form collicular vein (Figs. 24, 26). The collicular vein collects the venous blood from both colliculi into the rectus sinus. In some cases, it drains the blood into the confluence sinus and then to the transverse sinus and finally to the external jugular vein mostly and some into the internal jugular vein (Fig. 47).

Moreover, the venous drainage of the midbrain could be divided into three major groups according to the areas of drainage. The anterior or petrosal group is formed by the veins draining anteriorly into superior petrosal sinus. The second is the superior or galenic group that is the veins converging on the great vein of Galen and

the posterior group is the third group which drains into the transverse or rectus sinuses (Fig. 47). In common tree shrew, the veins at the ventral aspect of the midbrain are the posterior communicating, peduncular, anterior mesencephalic veins and the vein of pontomesencephalic sulcus. They drain the blood into the basal vein and then empty into the superior petrosal sinus that is the first group. The thalamocollicular vein that receives the venous blood from the internal part especially the dorsal part of cerebral aqueduct drains the venous blood into the great vein of Galen that is the second groups of venous drainage. The last group could be demonstrated in the caudal midbrain. The collicular or quadrigeminal vein empty directly into the transverse or rectus sinuses.

Figure 1. Photograph of the common tree shrew brain, top view, after removal of the left cerebral hemisphere, showing the superior colliculus (SC) and the related structures. Th, thalamus; CbC, cerebral cortex; Cbl, cerebellum.

Figure 2. Photograph of the common tree shrew brain, ventral aspect, showing pons (P), mammillary body (Mb), metathalamus (Met), optic tract (OT), interpeduncular fossa (asterisk) and oculomotor nerve (arrowhead).

Figure 3. Photograph of the midsagittal section of the common tree brain showing the midbrain and related structures. SC, superior colliculus; IC, inferior colliculus; Teg, tegmentum; asterisk, interpeduncular fossa; Th, thalamus; P, pons; CbC, cerebral cortex; Cbl, cerebellum.

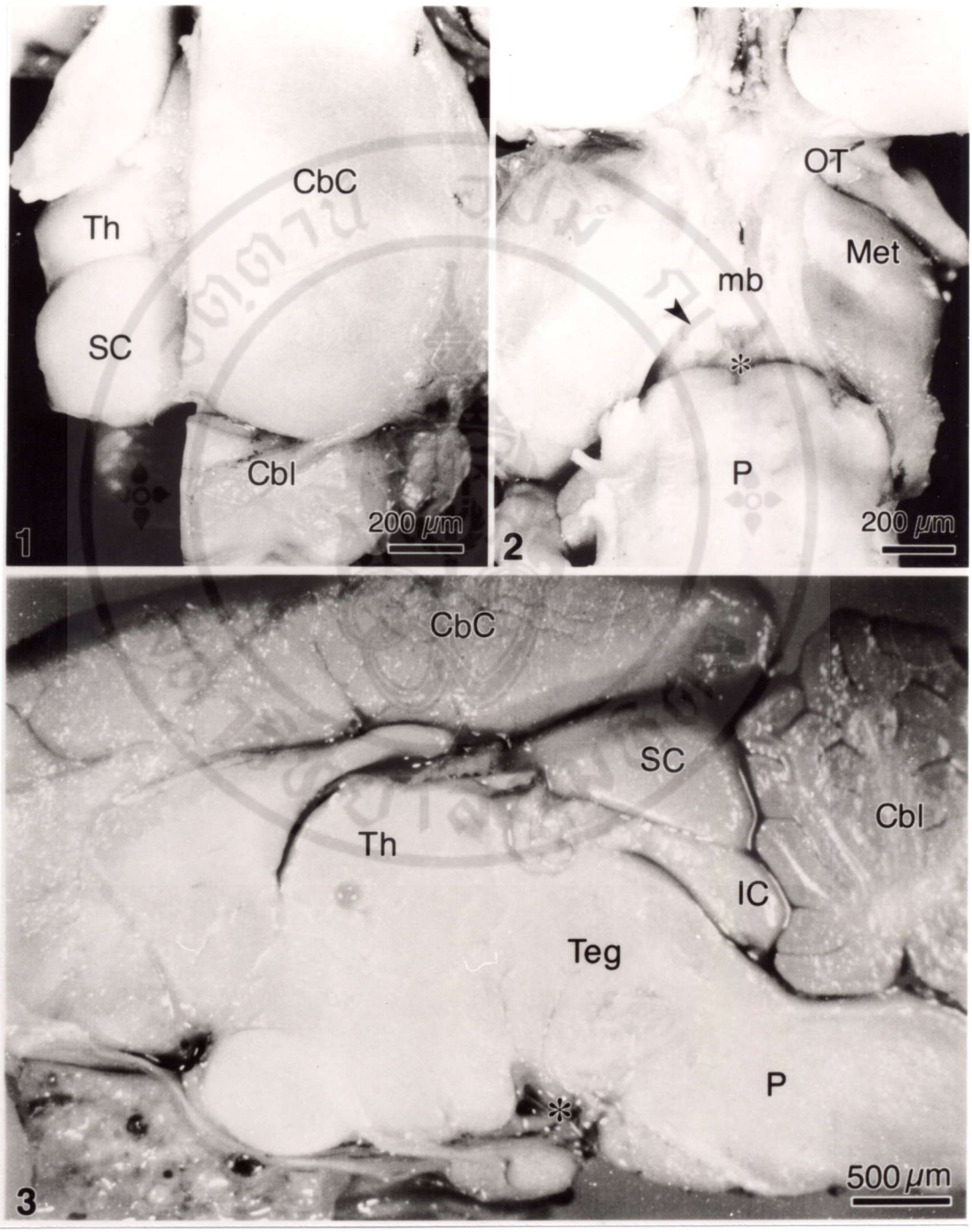

Figure 4. Light micrograph of the intermediate midbrain, cross section, showing the three major regions. Tec, tectum; Teg, tegmentum; asterisk, crus cerebri.

Figure 5. Light micrograph of the midbrain, cross section, showing the six cytoarchitectural subdivisions of superior colliculus. 1, stratum zonale; 2, stratum griseum superficiale; 3, stratum opticum; 4, stratum griseum intermediale; 5, stratum album intermediale; 6, stratum griseum profundum; arrowhead, optic tract.

Figure 6. Light micrograph of the caudal midbrain, cross section, showing the subdivision of the inferior colliculus. ICC, central nucleus of the inferior colliculus; open arrowhead, pericentral nucleus; asterisk, external nucleus; SC, superior colliculus; P, pons.

Figure 7. Light micrograph of the intermediate midbrain, cross section, showing red nucleus (R) and substantia nigra (SN). MGB, medial geniculate body; asterisk, interpeduncular nucleus.

Figure 8. Light micrograph of the intermediate midbrain, cross section, showing the oculomotor nuclear complex (Oc) and oculomotor nerve (open arrowhead). Arrowhead, mesencephalic nucleus of trigeminal nerve.

Figure 9. Light micrograph of the transactional section of superior and inferior colliculus midbrain, cross section, showing the trochlear nerve nucleus (Tr). DSCP, decussation of the superior cerebellar peduncles; CG, central gray; asterisk, medial longitudinal fasiculus.

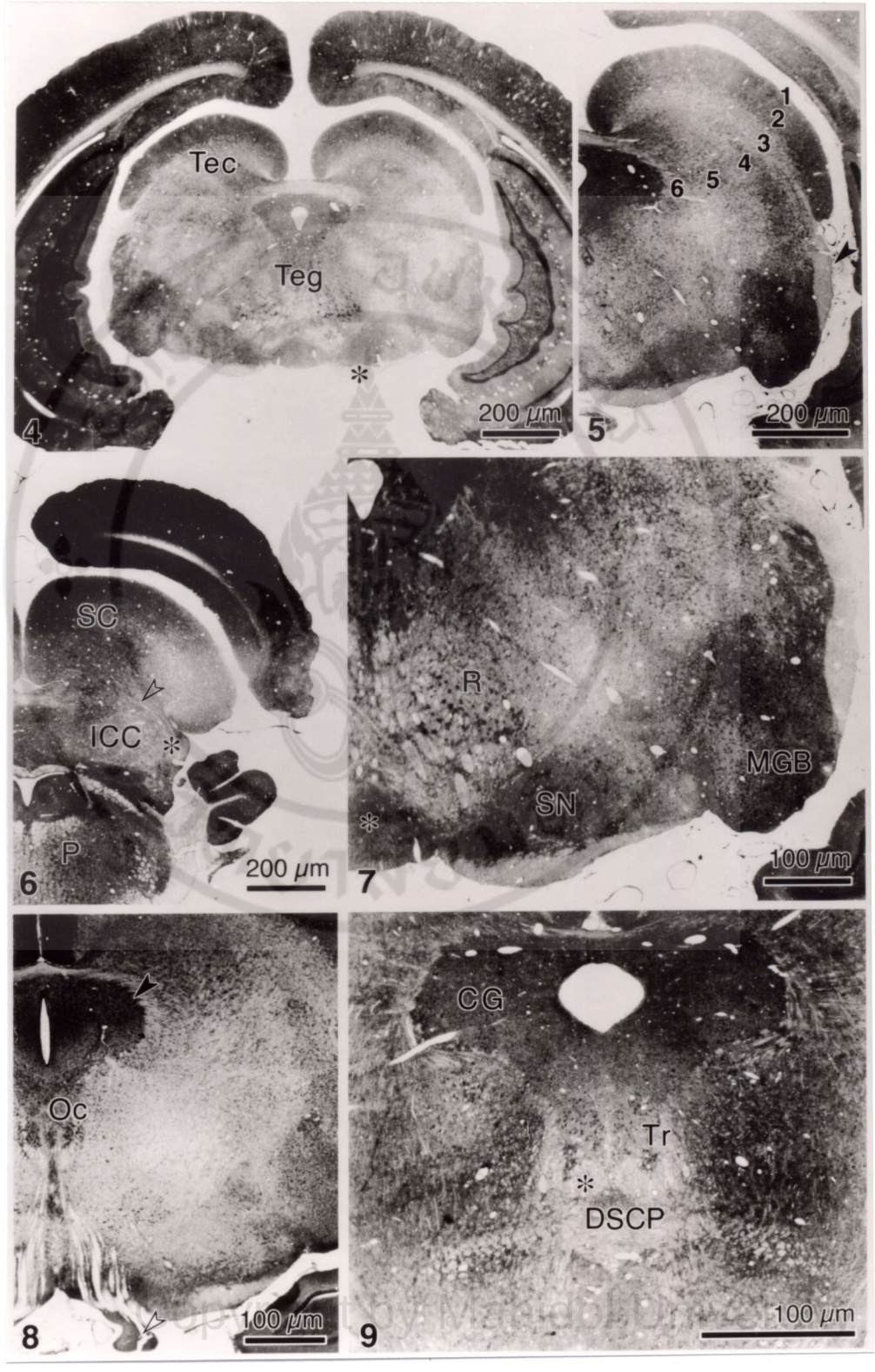
Tec
Teg
200 μm
4
1
2
3
4
5
6
200 μm
5
SC
ICC
P
200 μm
6
R
SN
MGB
100 μm
7
Oc
100 μm
8
CG
Tr
DSCP
100 μm
9

Figure 10. Photograph of the arterial system supplying the brain of the common tree shrew. 1, vertebral artery; 2, basilar artery; 3, internal carotid artery; 4, posterior cerebral artery; 5, superior cerebellar artery; 6, posterior communicating artery; 7, middle cerebral artery; 8, anterior communicating artery; asterisk, basilar artery bifurcation and its perforating branches.

Figure 11. Stereomicrograph of the cross section of the vascular casts, showing four groups of penetrating arteries of the midbrain as anteromedial (A), anterolateral (B), lateral (C) and posterior groups (D).

Figure 12. Stereomicrograph of the vascular corrosion cast, midsagittal section, showing the paramedian thalamomesencephalic arteries (asterisks).

10

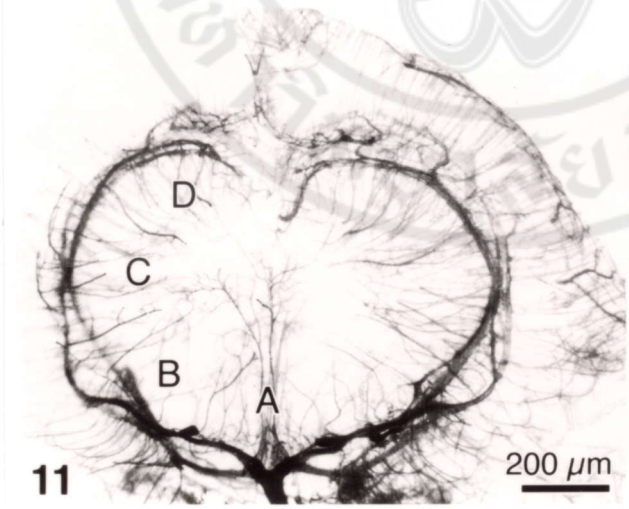

11

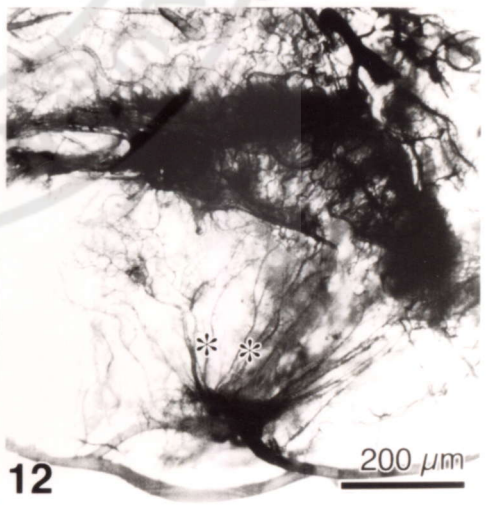

12

Figure 13. Stereomicrograph of the vascular casts of the midbrain, dorsal aspect, showing the superior colliculus (SC) and its blood supply. Th, thalamus; 3VCP, choroid plexus of third ventricle; arrowhead, medial posterior choroidal artery.

Figure 14. Stereomicrograph of the vascular casts of the midbrain, ventral aspect, showing the main arterial supply of the midbrain. Asterisk, basilar artery bifurcation; 1, basilar artery; 2, superior cerebellar artery; 3, posterior cerebral artery.

Figure 15. Stereomicrograph of the vascular casts of the midbrain, ventrolateral aspect, showing the posterior cerebral artery (arrowhead). IC, inferior colliculus; LVCP, choroid plexus of lateral ventricle; Th, thalamus.

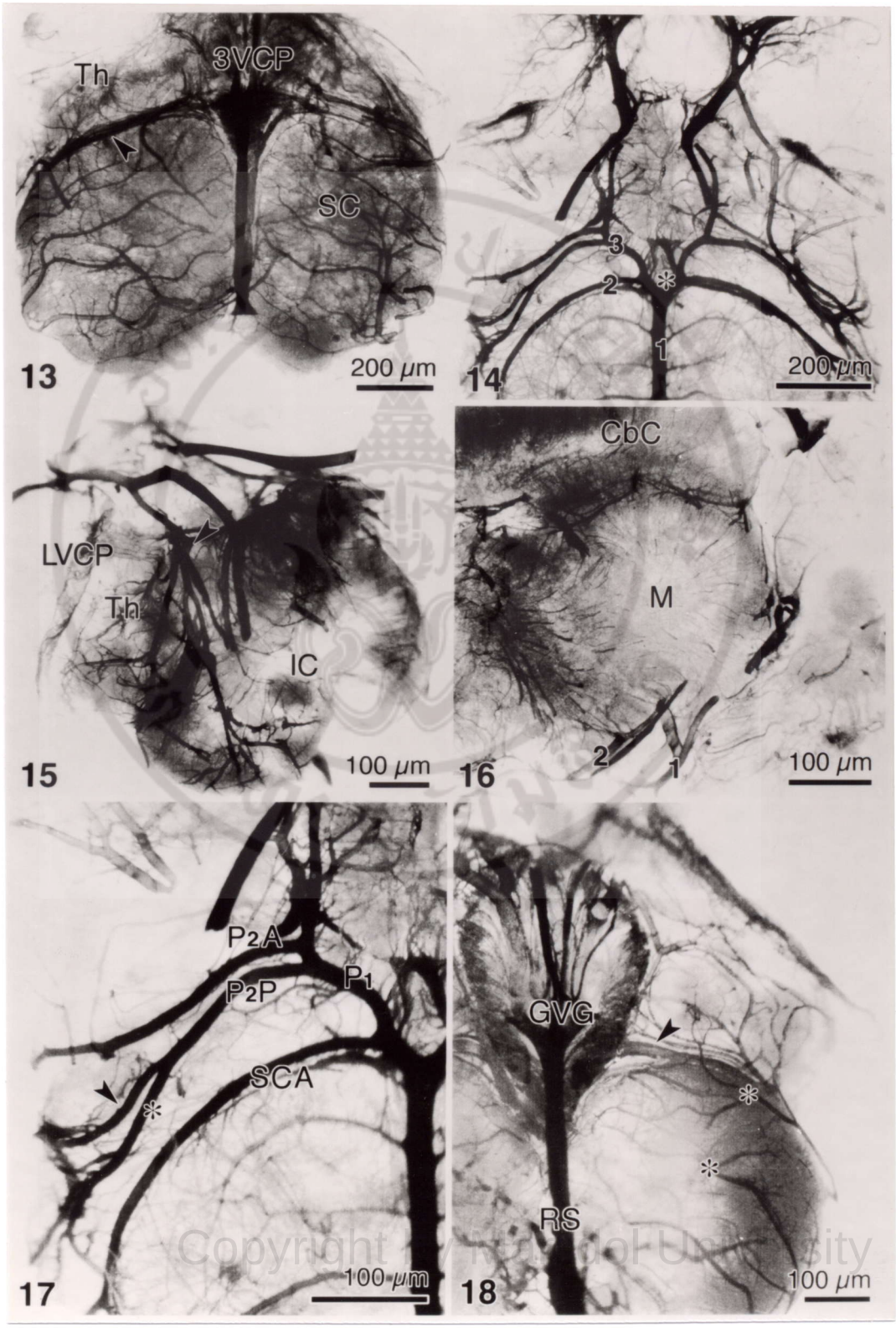

Figure16. Stereomicrograph of the vascular casts of the midbrain, parasagittal section, showing the penetrating arteries supplying the internal part of the midbrain (M). 1, superior cerebellar artery; 2, posterior cerebral artery; CbC, cerebral cortex.

Figure 17. Stereomicrograph of the vascular casts of the midbrain, ventral aspect, at the higher magnification, showing the subdivision of the posterior cerebral artery. P1, first part of the PCA; P2A, anterior half of the second part of posterior cerebral artery; P2P, posterior half of the second part of posterior cerebral artery; SCA, superior cerebellar artery; arrowhead, medial posterior choroidal artery; asterisk, collicular artery.

Figure 18. Stereomicrograph of the vascular casts of the midbrain, dorsal aspect, at higher magnification, showing the branches of the collicular artery (asterisks) supplying the tectum. arrowhead, thalamocollicular vein; GVG, great vein of Galen; RS, rectus sinus.

Figure 19. Light micrograph of the rostral midbrain, cross section, showing the superior colliculus (SC), red nucleus (R), substantia nigra (SN), pineal gland (Pi) and oculomotor nerve (N III).

Figure 20. Stereomicrograph of the vascular casts of the midbrain, at the similar level to that in Figure 19, showing the vascular supply the rostral midbrain. P1, first part of posterior cerebral artery; P2, second part of posterior cerebral artery; SC, superior colliculus; arrow, medial posterior choroidal artery.

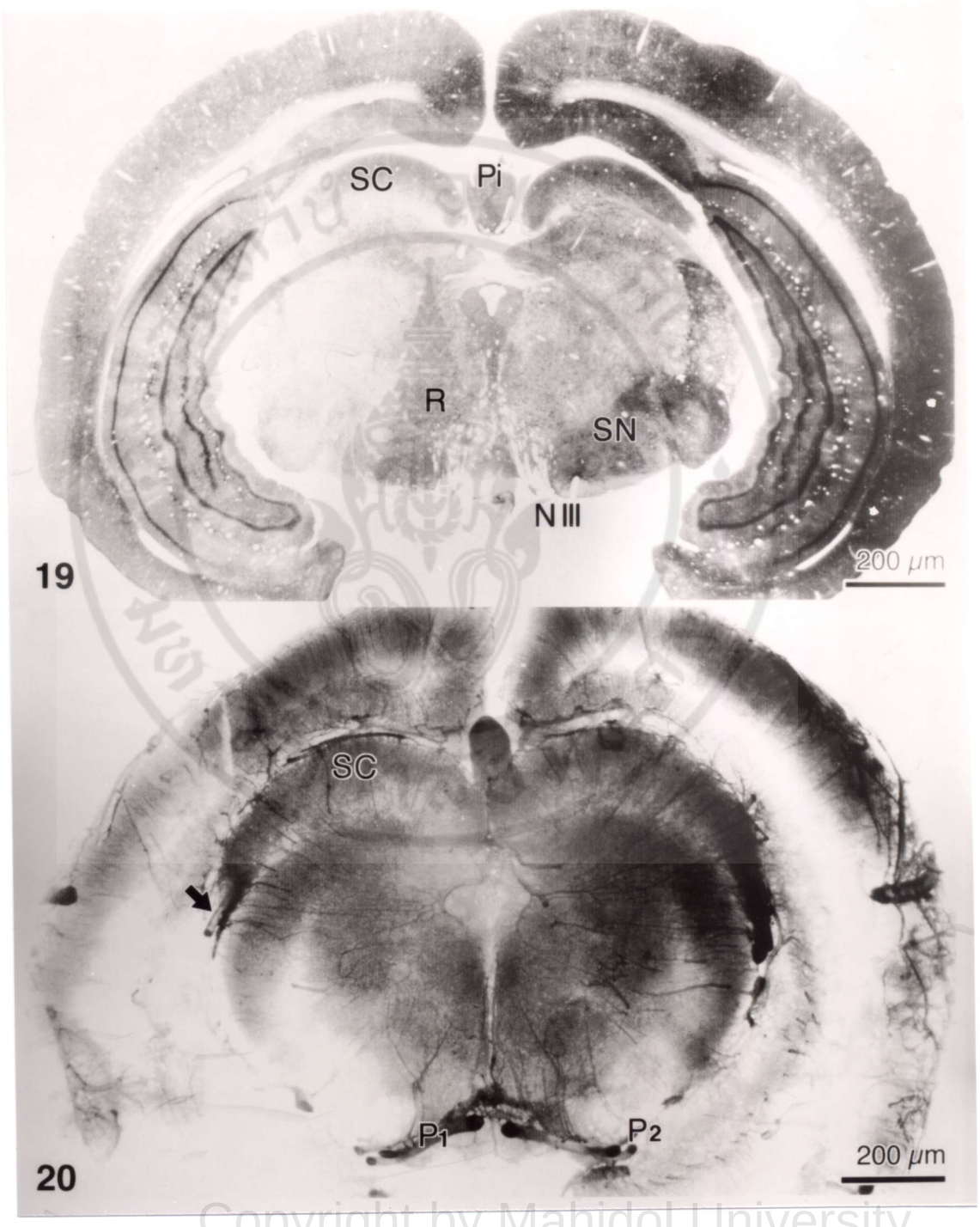

Figure 21. Light micrograph of the intermediate midbrain, cross section, showing the superior colliculus (SC), oculomotor nuclear complex (Oc), red nucleus (R) and interpeduncular nucleus (Ip).

Figure 22. Stereomicrograph of the vascular casts of the midbrain, at the similar level to that in Figure 21, showing the arterial supply the superior colliculus (SC) and oculomotor nuclear complex (Oc). Asterisk, anteromedial arteries; open arrowheads, anterolateral arteries; BA, basilar artery.

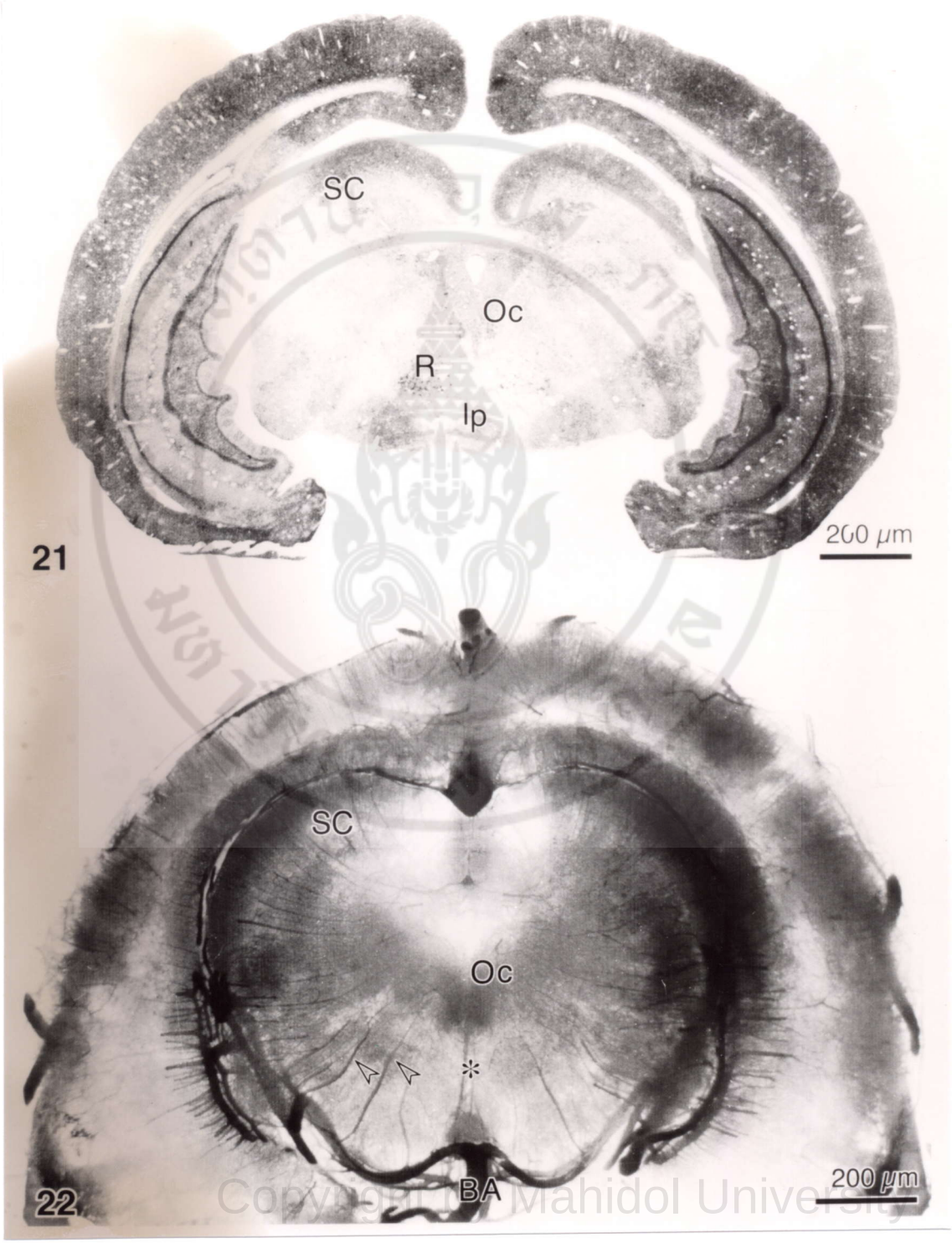

Figure 23. Light micrograph of the caudal midbrain, cross section, showing the central nucleus of inferior colliculus (ICC), superior colliculus (SC), pons (P) and trochlear nerve (open arrowhead).

Figure 24. Stereomicrograph of the vascular casts of the midbrain, at the similar level to that in Figure 23, showing the dense vascularity in the central nucleus of inferior colliculus (ICC), collicular vein (asterisk), transverse sinus (TS) and superior petrosal sinus (SPS).

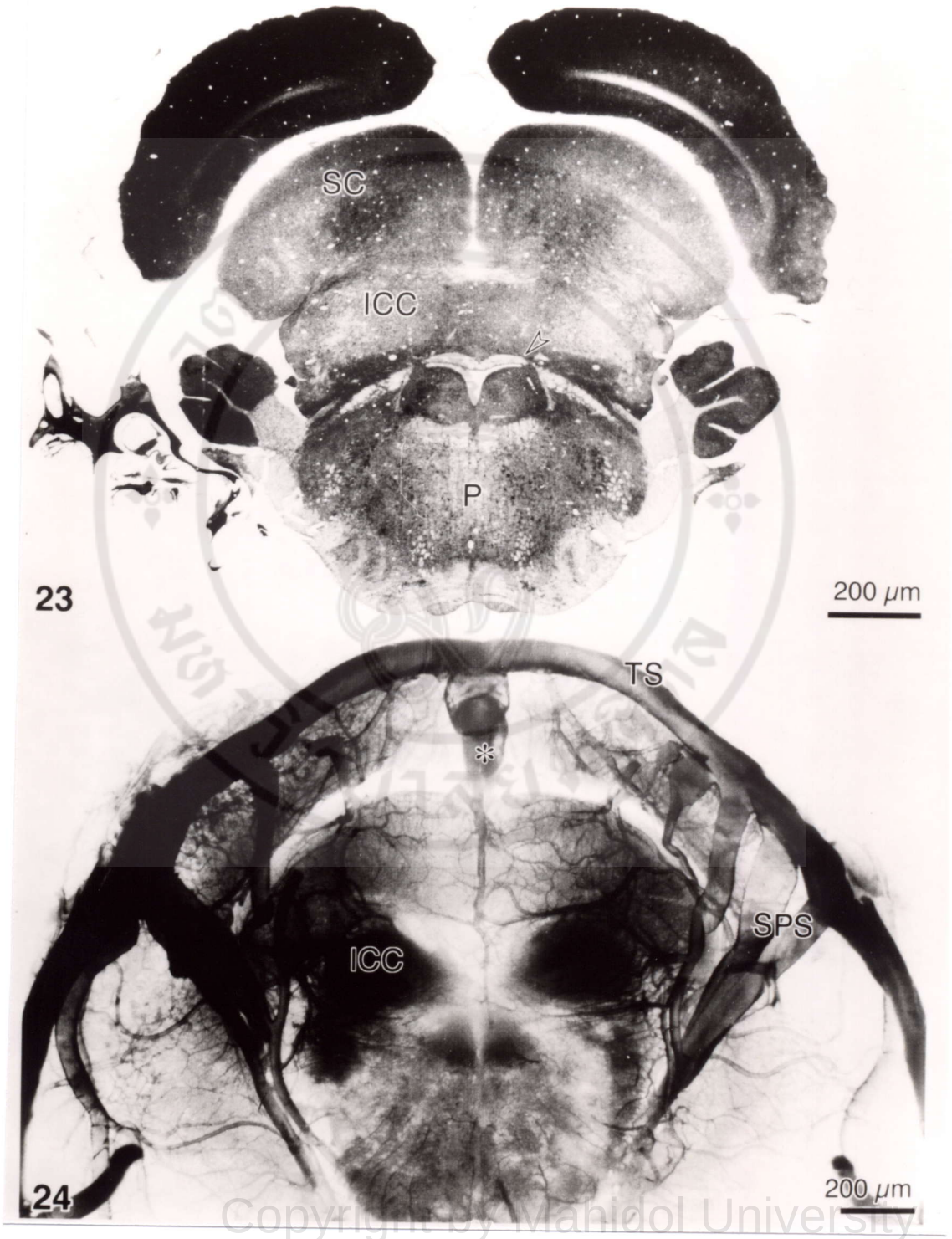

Figure 25. Stereomicrograph at high magnification of the vascular casts of the mid area of midbrain, cross section, showing the posterior group of the penetrating arteries supplying the superior colliculus. 1, superficial layer; 2, deep layer; 3, central gray layer; open arrowhead, dorsal aqueductal vein; asterisk, anteromedial artery; RS, rectus sinus.

Figure 26. Stereomicrograph of the vascular casts of the midbrain, midsagittal section, showing the paramedian thalamomesencephalic arteries (asterisk) supply the oculomotor nuclear complex (Oc) and Trochlear nucleus (Tr). Open arrowhead, dorsal aqueductal vein, arrowhead, lateral aqueductal vein; GVG, great vein of Galen; RS, rectus sinus; CV, collicular vein; BA, basilar artery; Cbl, cerebellum; P, pons.

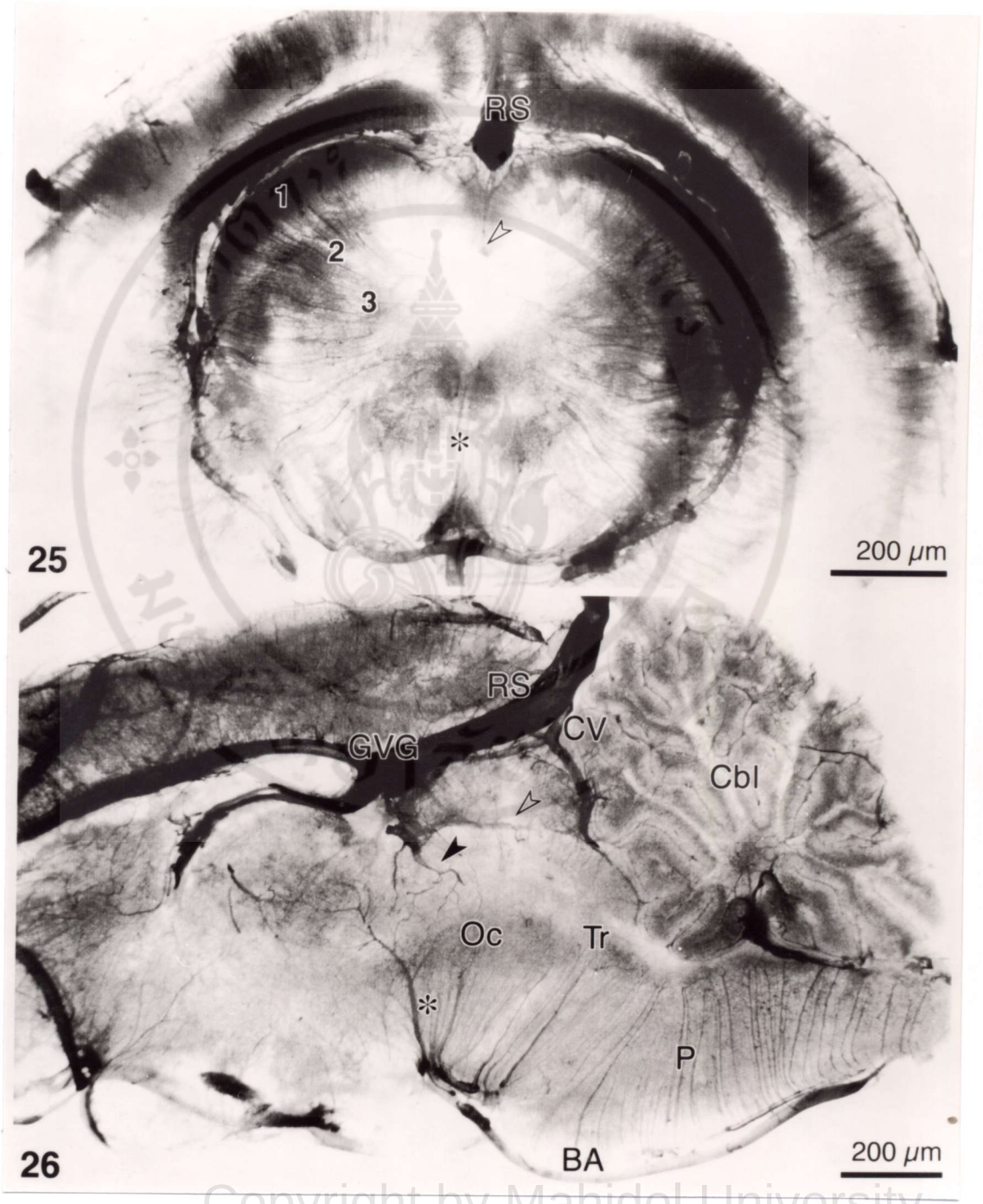

Figure 27. Stereomicrograph at the higher magnification of the vascular casts, cross section of the intermediate midbrain, showing the blood supply the midbrain nuclei, oculomotor nuclear complex (Oc), red nucleus (R), interpeduncular nucleus (Ip), superior colliculus (SC). Arrowhead, collicular artery; open arrowhead, lateral arteries; asterisk, lateral aqueductal vein.

Figure 28. Stereomicrograph at the higher magnification of the vascular casts of the intermediate midbrain, cross section, showing the anteromedial (asterisk) and anterolateral (open arrowhead) arteries supplying red nucleus (R). CA, cerebral aqueduct; P2A, anterior half of the second part of posterior cerebral artery; P2P, posterior half of the second part of posterior cerebral artery; Oc, oculomotor nuclear complex.

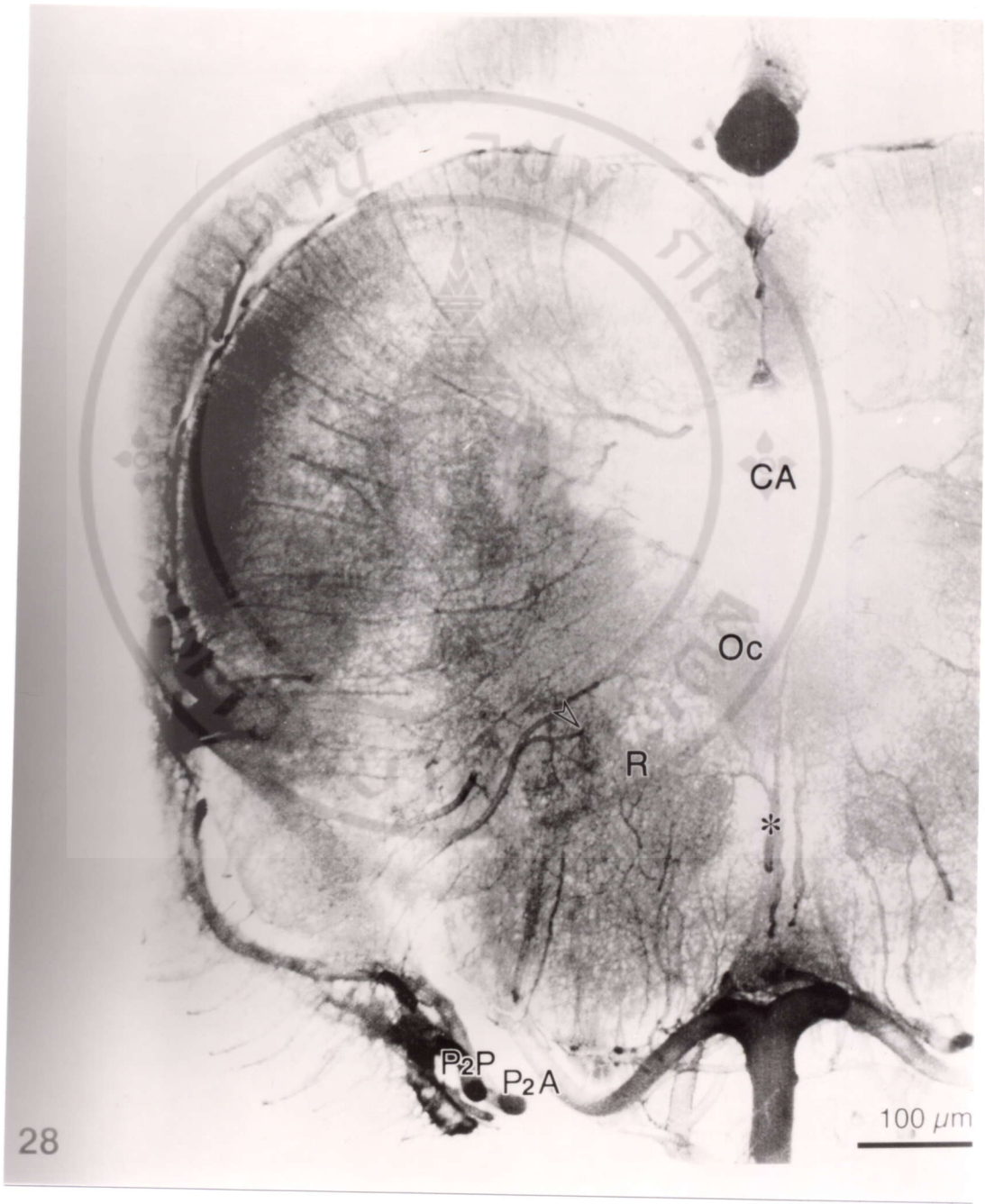

Figure 29. SEM micrograph of the vascular casts, ventral aspect of the midbrain showing the basilar artery (BA) and its branches. SCA, superior cerebellar artery; asterisks, perforating branches of the basilar bifurcation; Mb, mammillary body; P1, first part of posterior cerebral artery; arrowhead, peduncular branch; open arrowhead, vein of pontomesencephalic sulcus.

Figure 30. SEM micrograph of the vascular casts of the lateral aspect of the midbrain, showing the first part of posterior cerebral artery (P1) and second part of posterior cerebral artery (P2). Arrow, medial posterior choroidal artery; CA, collicular artery.

Figure 31. SEM micrograph of the vascular casts of the midbrain, cross section, showing the three layers of the vascular supply the superior colliculus. 1, superficial layer; 2, deep layer; 3, central gray layer.

Figure 32. SEM micrograph of the vascular casts at the surface of the midbrain showing the artery (A) giving off the penetrating arteries (arrowhead). Cp, capillary plexus; V, veins.

Figure 33. SEM micrograph of the vascular casts, at the higher magnification, showing the arterial anastomoses (asterisk) and the penetrating artery (arrowhead). V, vein.

Figure 34. SEM micrograph of the vascular casts of the lateral aspect of the midbrain, showing the medial posterior choroidal artery (asterisk) that accompanied by the thalamocollicular vein (ThCV) and drain the venous blood into the basal vein (BV).Note the vein (V) has a larger diameter than the accompany artery (A).

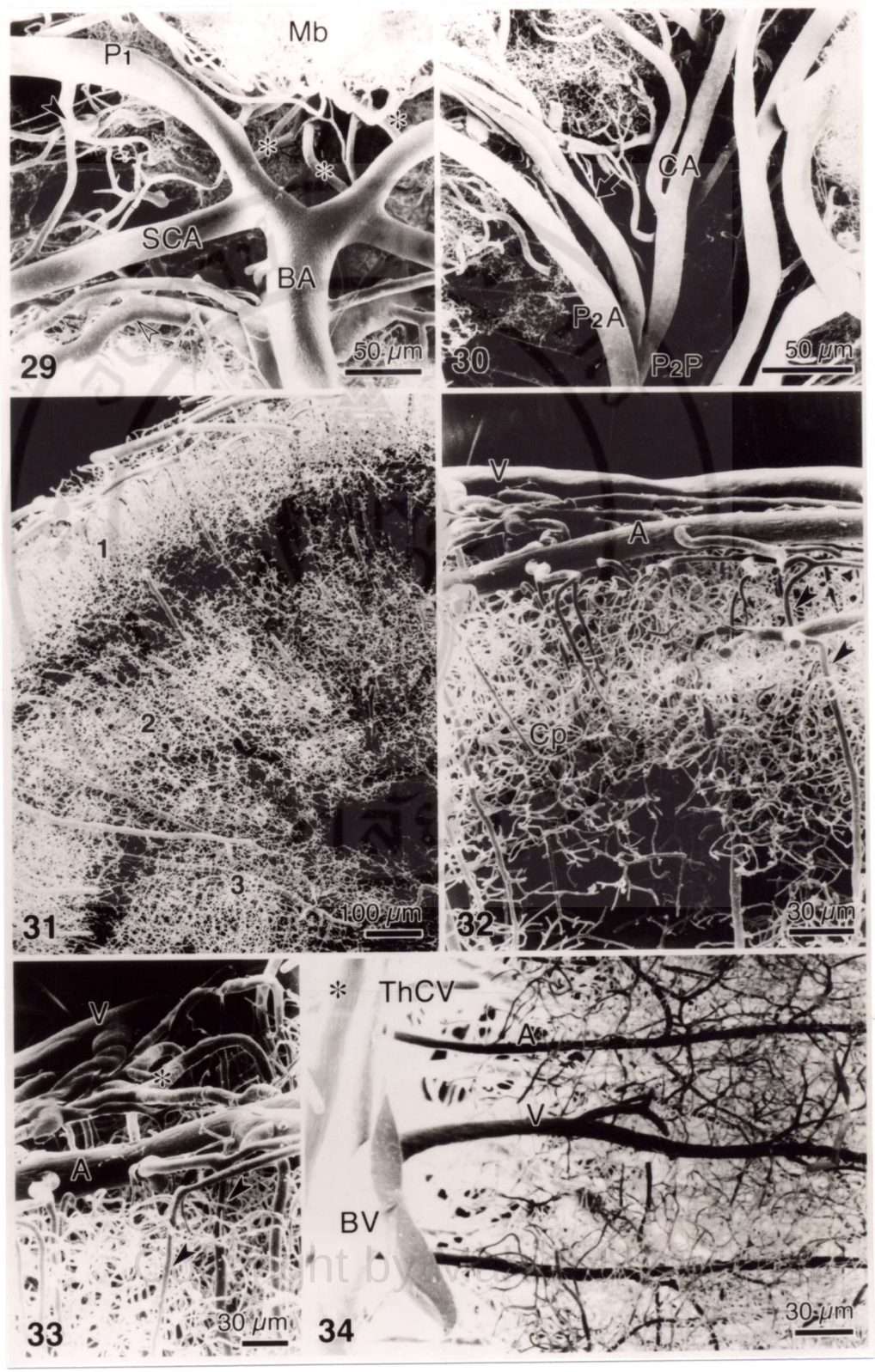
Mb
P1
SCA
BA
50 μm
29
CA
P2A
P2P
50 μm
30
1
2
3
100 μm
31
V
A
Cp
30 μm
32
V
A
30 μm
33
ThCV
A
V
BV
30 μm
34

Figure 35. SEM micrograph of the vascular casts of the dorsal aspect of the midbrain, showing the arterial anastomoses (asterisks) of the collicular arteries (arrowhead) on the surface of the quadrigeminal plate.

Figure 36. SEM micrograph of the vascular casts, cross section, the ventral aspect of the midbrain, showing the paramedian arteries (arrowheads) accompanying the paramedian veins (arrow). Asterisk, arterial anastomoses; PCoV, posterior communicating vein. Note dense capillary networks in the area of red nucleus (R).

Figure 37. SEM micrograph of the vascular casts showing veins of the ventral aspect of the midbrain. PCoV, posterior communicating vein; arrow, anterior mesencephalic vein; asterisk, peduncular vein; BA, basilar artery.

Figure 38. SEM micrograph of the vascular casts, cross section, showing the venous drainage from the dorsal part of cerebral aqueduct (CA). Arrow, dorsal aqueductal vein; asterisk, collicular vein; RS, rectus sinus; SC, superior colliculus.

Figure39,40. SEM micrograph of the vascular casts showing the density of the capillary networks (Cp) in the areas of the midbrain nuclei (Figure 39) comparing with the area of nerve fiber (Figure 40).

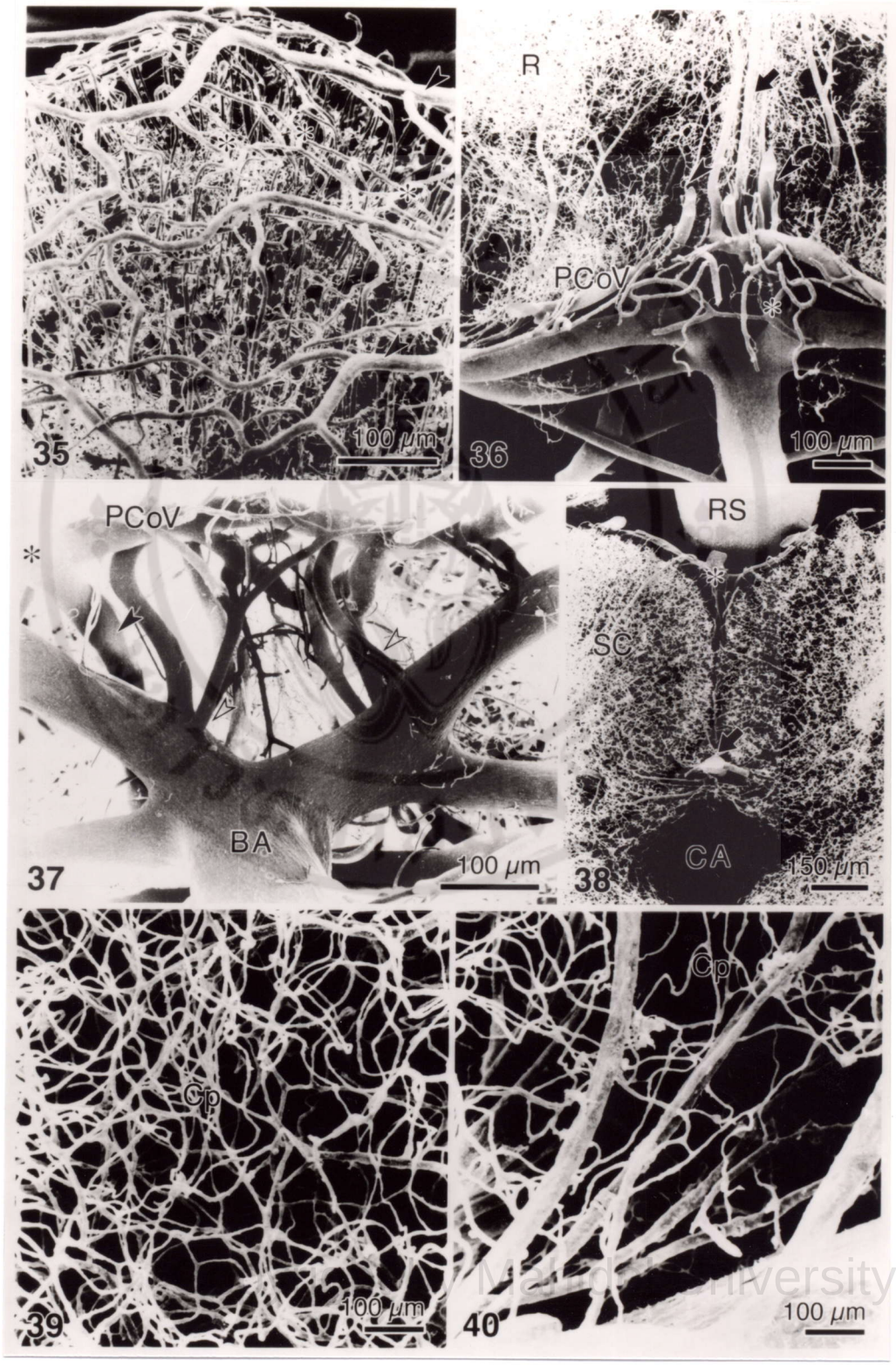

Figure 41. SEM micrograph of the vascular casts demonstrating the artery (A) at the surface of the midbrain giving off the penetrating artery (a) that rapidly reduce in diameter. Arrowhead, arterial sphincter; Cp, capillary plexus.

Figure 42. SEM micrograph of the vascular casts of the internal artery of the midbrain showing the arterial sphincter (arrowhead).

Figure 43. SEM micrograph of the vascular casts showing the smooth muscle cells (open arrowheads) wrapping around the artery.

Figure 44. SEM micrograph of vascular casts showing the capillary connection (asterisks) continuing to the large venule (v).

Figure 45. SEM micrograph at higher magnification of the vascular casts illustrating the non-fenestrated capillary in the midbrain.

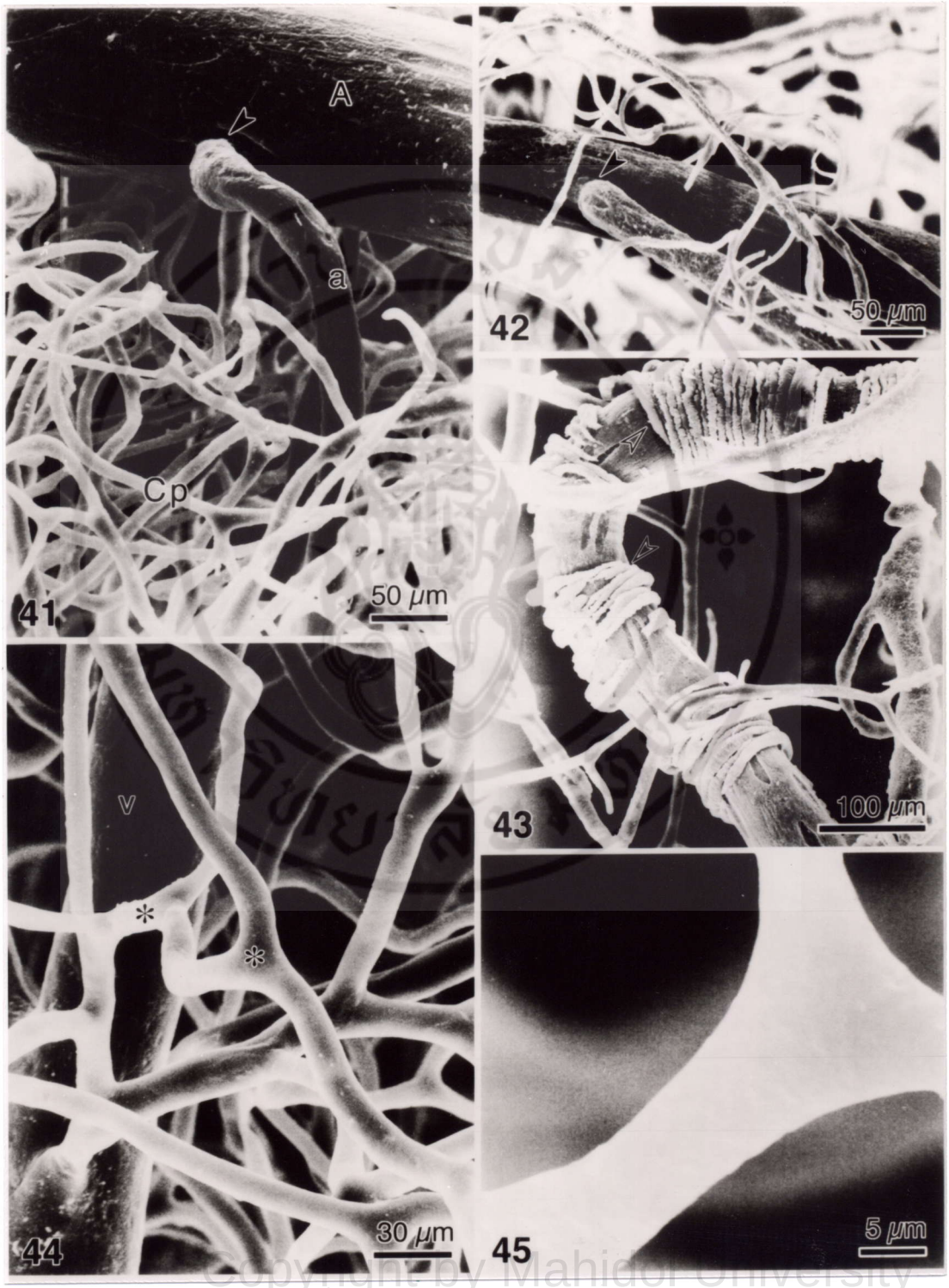

Figure 46. Diagram of the common tree shrew brain illustrating the arterial supply of the midbrain. BA, basilar artery; ICA, internal carotid artery; star, basilar artery bifurcation and its perforating branches; 1, first part of posterior cerebral artery; 2, posterior half of the second part of posterior cerebral artery; 3, anterior half of the second part of posterior cerebral artery; 4, superior cerebellar artery; 5, collicular arteries; 6, medial posterior choroidal artery; arrowhead, collicular branch of superior cerebellar artery; P, pons; Cbl, cerebellum; Th, thalamus; CbC, cerebral cortex.

Figure 47. Diagram of the common tree shrew brain illustrating the venous drainage of the midbrain. 1, anterior pontomesencephalic vein; 2, posterior communicating vein; 3, peduncular vein; 4, anterior mesencephalic vein; 5, basal vein; 6, superior petrosal sinus; 7, thalamocollicular vein; 8, dorsal aqueductal vein; star, great vein of Galen; open arrowhead, collicular vein; arrow, anterior mesencephalic vein; SSS, superior sagittal sinus; ISS, inferior sagittal sinus; RS, rectus sinus; ICV, internal cerebral vein; TS, transverse sinus; SS, sigmoid sinus; IJV, internal jugular vein; EJV, external jugular vein.

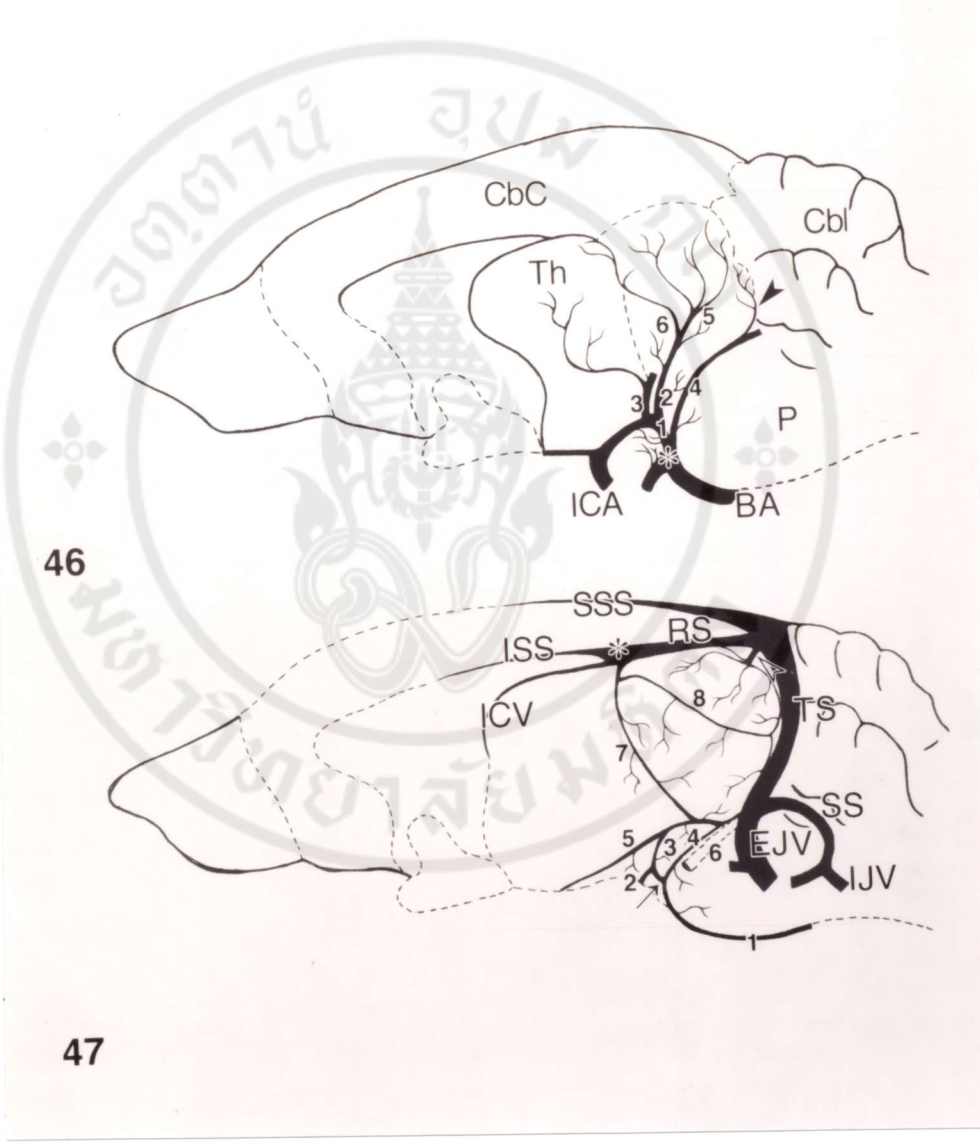

CHAPTER VI

DISCUSSION

The Anatomy of the Midbrain

In common tree shrew, the midbrain or mesencephalon is relatively very large when compares to the whole brainstem. It is covered by the expanded occipital pole, so that it is not visible from the dorsal aspect. This feature is common in all mammalian members of Orders Marsupialia, Rodentia, Lagomorpha and Primates (71). The internal structure of the common tree shrew midbrain could be divided into tectum, tegmentum and basis as in other mammals (72) and man (20, 22, 23, 24). The tectum or roof consists of superior and inferior colliculi. The superior colliculus in the tree shrew is remarkably large and well developed with distinctively differentiated layers (73, 74, 75). The laminated organization of the superior colliculus in *Tupaia glis* has been studied by many authors basing on the cytoarchitecture, afferent connection (73, 74, 75, 76) and receptive field properties (77, 78, 79). Various authors subdivided the superior colliculus into seven to nine layers by modifying from the pattern of six layers appearing in other vertebrates. The lamination of superior colliculus is formed during embryonic development. The cells migrate toward periphery from the periventricular mass and the successive layers are occurring (80). In *Tupaia glis*, there is the superficial gray layer as in mammals but not in nonmammalian vertebrates (2, 80). Among mammals, the best developed with very distinct layers could be observed in common tree shrew as well as in gray squirrels

(81), rat (82) and cat (83). However, the layers in tree shrew are more clearly depicted. The extremely large superior colliculus in the tree shrew could associate with compensative function for a poor-developed cerebellum. In addition, this well-developed organ could very well relate with effective visual system in order to achieve its arboreal habitat (18). The relative size and differentiation of the superior colliculus is not certain among mammalian Orders. It is very large in flying lemur, squirrel and tree shrew. These animals have common rapid locomotive behavior and with arboreal niche. In prosimian and insectivore, the superior colliculus is relatively small and less differentiated. Eventhough, the superior colliculus of the lemur is smaller than in tree shrew, this animal is with highly visual activity (75). The size of the superior colliculus among the closely related species has been supported to be correlated with different ecological requirements (74).

Unlike in nonmammalian vertebrates, the torus semicircularis (inferior colliculus) lies ventrally to the optic tectum (superior colliculus) because of the lateral expansion of the optic tectum with the tectal ventricle formation. The subdivisions of the inferior colliculus in *Tupaia glis* are quite similar to those in the cat (84, 85) and man (21) being the central, pericentral and external nuclei (84).

It is quite interesting that the tegmental nuclei of the common tree shrew concerning with the visual function are well developed. These nuclei are the oculomotor, trochlear and the Edinger-Westphal nuclei. The red nucleus in the tree shrew is an egg-shaped structure as seen in other mammals (72, 86, 87). The interpeduncular nucleus situates in the midline above the interpeduncular fossa (IF). This nucleus extends from the caudal pole of the mammillary body to the beginning of

the pontine gray. This feature is also exhibited in rodent (88), shrew, bat (89), dog and cat (90). In monkey and man, the whole mass is relatively small (72). The substantia nigra (SN) in the tree shrew could also be divided in zona or pars compacta, recticulata and lateralis as observed in other mammals (72, 88, 89, 90, 91, 92, 93, 94, 95, 96). The melanin pigment is seen in the nigral cells as in other mammalian Orders. However, there is less number of pigmented cells with minimal number of pigmented granules in each cell of the tree shrew substantia nigra. In Primates, the intensity of pigmentation increases when the animals are genetically close to man (97). The crus cerebri in *Tupaia glis* is less developed and relatively small when compare with other parts of the midbrain.

It is obvious that the mainly histological features of the midbrain in common tree shrew are quite similar to those of other mammals, especially primates. However, the large size of the superior colliculus indicates that the tree shrew brain has some primitive features when compare with other primates (18).

The Midbrain Vascularization

In general, the organization of the major cerebral arteries of the brain in common tree shrew is similar to that in man (64). These branches are from the internal carotid (ICA) and the vertebrobasilar systems that form complete circle of Willis. There is anterior communicating artery in the common tree shrew as in man (98, 99) but not in rat (98), opossum, armadillo (4), baboon and vervet monkey (100). It is obvious that the arterial circle of Willis in common tree shrew is quite similar to that of man than these in the rat and other primates. The main sources of the arterial supply

to the midbrain in common tree shrew are from the branches of the vertebrobasilar system. They are basilar bifurcation, posterior cerebral, superior cerebellar, medial posterior choroidal and collicular arteries. These are principally similar to those of man (1, 5, 7, 26), guinea pig (13, 14) and dog (11, 12). As the midbrain receives the blood from many sources and the midbrain in common tree shrew is very large, the organization of the blood vessels in this organ is very complex and quite different from other animals. The area distribution could correspond to the sources of the arterial supply. In the submammalian vertebrates as in fishes, amphibians, reptiles and bird, their midbrains are supplied by branches from the caudal division of the internal carotid artery (ICA) (3). However, the crus cerebri of the midbrain in the guinea pig (14), dog (12) and some cases of human (7, 48, 101), but not in common tree shrew, receives the blood supply from the posterior communicating artery (PCoA). In anuran, the midbrain is supplied by the superior mesencephalic artery that arises from the posterior ramus of the ICA (66) as in the case of other submammalian vertebrates (3). In many higher mammals (3, 8, 10, 11, 12, 13, 14) and man (102, 103) as well as in tree shrew, the posterior cerebral artery (PCA) is the major source of blood supply to the midbrain. This artery in the rat (98) and man (5, 28, 30, 104) usually originates from the basilar artery (BA). It is noted that the symmetrical appearance of the PCA could be observed. In human embryo, the PCA arises as a branch of ICA (25, 26, 28). Stephens and Stilwell (5) proposed that the PCA would be a unique artery as it receives the blood from the basilar artery (BA) but originates from the ICA.

The PCA in common tree shrew could be divided into four segments as in man (28, 30, 42). However, there is some difference from the cases of man that the

collicular artery in the tree shrew does not come from the P1 segment (7, 28). In some cases, there is the accessory collicular artery branching from the P1 segment. The P1 segment of the PCA or basilar communicating artery or mesencephalic artery is the segment that situates between the proximal portion of the PCA extending from the basilar bifurcation to PCoA (5, 25, 26, 28, 30, 35, 39, 105). The term of mesencephalic artery could not be acceptable because of it gives the branches to supply both the midbrain and the thalamus. The infarction occurring in this territories generally results in the mesencephalothalamic syndrome (106, 107, 108).

Most of the arteries that supplying the midbrain in common tree shrew are the branches from the rostral part of the vertebrobasilar system. They give the direct perforating arteries in the interpeduncular fossa and supply the midline region. Then they send the short and long branches encircle the midbrain and give the smaller branches to penetrate the midbrain at right angle into the tissue and reach the cerebral aqueduct. The penetrating arteries exhibit the radial pattern as appears in man (5, 25, 36, 47), guinea pig (13, 14), dog (11, 12), anuran (66) and submammalian vertebrates (3). The general radial pattern of the internal vascularity as seen in the midbrain of the common tree shrew could be observed in all vertebrates including primates.

The pattern of vascular arrangement within the midbrain has been described in man (5, 7, 36, 109), dog (11, 12) and guinea pig (14) as same as in this studies, the arterial supply the common tree shrew midbrain could be divided into anteromedial, anterolateral, lateral and posterior groups according to their points of penetration and the territories that supply them. The origins of the arteries and the arterial vascular

territories in the midbrain and brainstem are the basic information leading to the understanding of various syndromes (6, 47, 109).

The anteromedial group consists of the direct perforating arteries branching from the tip of basilar artery, P1 segment of PCA and initial segment of SCA. They are the paramedian thalamomesencephalic arteries that originate from the parent arteries in the symmetrical fashion. This is different from man of which the main stems of the perforating artery are usually seen in the interpeduncular fossa (7, 29, 32, 33) but after penetrating into the internal part, a tendency to go to the right and left sides is rather symmetrical (110). The penetrating arteries in the anterolateral group do not reach the cerebral aqueduct. They extend as far as the lateral part of the red nucleus (41). The arteries of the posterior group supply large territories when compare with those of other groups. The internal arrangement of this group could be observed as capillary plexuses in many areas corresponding to the cytoarchitectonic strata of the superior colliculus. This is also evident in the cat (111), anuran (66) and man (5, 47). The superficial layer is with the highest vascular density of the capillary networks. The suggestion is made that a lot of numerous of neurons in this layer associates with the visual activities (73, 74, 77, 78, 112). It is evident that there is close relationship among cytoarchitecture , richness of the capillary networks and the neuronal activity.

As observed in the midbrain of man (7, 44) and the cat (113), the arterial anastomoses could be observed in the perimesencephalic part (pial or external part of the midbrain). Such the external arterial anastomoses could be well observed in the dorsal aspect especially in the area of tectum. This is also true in man (7, 44), cat (9), fish, bird and chicken (3), guinea pig (14) and anuran (66). Which could be the reason

why the infarction in this area is very rare (115). In the ventral aspect, as in the man (29, 47), the arterial anastomoses could be less frequently demonstrated among the direct perforating arteries in the interpeduncular fossa (IF). It is also noted that they are considerable amounts of arterial anastomoses on the surface of the cerebral cortex in the common tree shrew (62) and rarely seen in thalamus (115). It is reasonable as the surface area of cerebral cortex is relatively large while that of the thalamus is rather small but the thalamus receives blood supply from branches of both ICA and the vertebrobasilar systems. It should be noted that the arterial anastomoses in the internal part of the midbrain in the common tree shrew could not be observed. The penetrating arterioles terminate into capillary networks as observed in all mammals, especially, in the primates. In opossum and marsupial, however, the capillary networks are not present. Instead, the capillary loops are found (4, 116).

The smooth muscle cells wrapping around the artery including the arteriolar and precapillary sphincters are usually found in the midbrain as well as in the thalamus (115) and in the human cerebral cortex (55, 56). These features could be participated in the regulating of blood flow into the capillary networks. As in the most parts of the tree shrew brain, the capillaries in the midbrain are without the fenestrations. However, the fenestrated capillaries in the tree shrew brain had been observed in choroid plexus (65), pineal gland (61) and pituitary gland (60). This type of capillaries has also been reported in the early developed chicken optic tectum (117).

With the light microscopic study of the midbrain paraffin sections in parallel to that of the sections of the midbrain vascular corrosion cast, it is obvious that the midbrain nuclei locate in the tegmentum are with a lot of blood supply. This finding is

also true in the dog (11) and the guinea pig (14). The dense vascularity could also be seen in the oculomotor nuclear complex, red nucleus, trochlear and interpeduncular nuclei. In pars compacta of SN, the capillary networks are much denser than those in other parts. This is quite similar to what has been reported in man (118), cat, monkey (119, 120) and primates (121). As in the rat (122, 123, 124), the central nucleus of inferior colliculus is with the greatest capillary density in the midbrain. The less vascularized areas are the crus cerebri and lateral part of the midbrain. These areas contain nerve fibers predominantly. It is quite certain that the degree of vascularity depends on the density of nerve cells.

The venous drainage of the midbrain in common tree shrew is quite similar to that in man (5, 50, 125, 126, 127, 128) but somewhat different from the guinea pig (14) and dog (11, 129). In man and in the common tree shrew, the venous drainage in the midbrain could be divided into anterior or petrosal, superior or galenic and posterior groups (130, 131). It is noted that the basal vein in common tree shrew drains the venous blood into both petrosal and galenic groups but dominantly into the great cerebral vein of Galen as in man (125, 127, 130, 131). However, in the dog, this vein drains mainly into the superior petrosal sinus (129). The collicular or quadrigeminal vein in the tree shrew collects the venous blood into the rectus sinus. This is different from man that this vein flows into the great vein of Galen (51, 127).

So far, the tree shrew (Tupaiidae) has been classified as a member of the Order Insectivores (17, 133) or of Order Primates (16, 19, 134, 135, 136, 137) while many authors suggest that it is a transitional form of mammal when basing on the neuroanatomical data of the visual pathway (18, 67, 68, 138, 139). In this study, the

anatomy and histology of the midbrain in common tree shrew (*Tupaia glis*) can not be used as good criteria to classify this animal as Insectivores, Primates or in a separate Order as Order Scandentia (140). However, this study indicates that the midbrain microvascularization in the common tree shrew (*Tupaia glis*) is very similar to that of higher primates.

CHAPTER VII

CONCLUSIONS

The microvascularization of the midbrain in common tree shrew (*Tupaia glis*) has been studied by vascular corrosion cast technique with stereomicroscope and scanning electron microscope (SEM). The findings are:

I. The arterial supply the midbrain

1. The blood supply the midbrain comes from the vertebrobasilar system and its branches. They are the basilar artery bifurcation, superior cerebellar, posterior cerebral, medial posterior choroidal and collicular arteries.

2. These arteries give off branches penetrating into the internal part of the midbrain in the radial pattern. It is the centripetal arrangement directing toward the cerebral aqueduct.

3. The penetrating arteries of the midbrain could be divided into anteromedial, anterolateral, lateral and posterior groups according to the points of penetration and the corresponding territories that they supply.

4. The arterial anastomoses could be observed in the perimesencephalic or pial or external part but not in the deep part of the midbrain.

5. The midbrain capillaries are without the fenestration.

6. The degree of vascularity in the midbrain is closely related to the density of nerve cells. The vascular density is high in the areas occupied by the midbrain nuclei and the low in the areas containing nerve fibers.

II. The venous drainage of the midbrain

1. The venous drainage could be divided into the anterior or petrosal group, the superior or galenic group and the posterior group.

2. The venous blood from the area ventral to the cerebral aqueduct is collected into the posterior communicating, peduncular and anterior mesencephalic veins that empty into the basal vein. The basal vein and the vein of the pontomesencephalic sulcus drain into the anterior or petrosal group.

3. The superior or galenic group receives the venous blood from the thalamocollicular vein, the lateral and dorsal aqueductal veins that drain into the great vein of Galen, rectus sinus, transverse sinus and finally into the external jugular vein predominantly.

4. The posterior group drains the venous blood from the superficial vein of the quadrigeminal plate and collicular veins into the rectus and transverse sinuses.

REFERENCES

1. Bogousslavsky J, Maeder P, Regli F, Meuli R. Pure midbrain infarction: clinical syndromes, MRI, and etiologic patterns. Neurology 1994; 44(11):2032-40.

2. Butler AB, Hodos W. Comparative vertebrate neuroanatomy: evolution and adaptation. New York: Wiley-Liss; 1996.

3. Gillilan LA. A comparative study of the extrinsic and intrinsic arterial blood supply to brains of submammalian vertebrates. J Comp Neurol 1967; 130(2):175-96.

4. Gillilan LA. Blood supply to primitive mammalian brains. J Comp Neurol 1972;45(2):209-22.

5. Stephens RB, Stilwell DL. Arteries and veins of the human brain. Springfield: Charles C Thomas; 1969.

6. Savoiardo M, Bracchi M, Passerini A, Visciani A. The vascular territories in the cerebellum and brainstem: CT and MR study. AJNR Am J Neuroradiol 1987;8(2):199-209.

7. Pullicino PM. The course and territories of cerebral small arteries. In: Pullicino PM, Caplan LR, Hommed M, editors. Advance in Neurology. Vol. 62. New York: Raven press; 1993.p.11-39.

8. Kanan CV. The cerebral arteries of *Camelus dronedarius*. Acta Anat (Basel) 1970;77(4):605-16.

9. Gillilan LA. Extra- and intra-cerebral blood supply to brains of dog and cat. Am J Anat 1976;146(3):237-54.

10. Anderson WD, Kubicek W. The vertebral-basilar system of the dog and relative to man and other mammals. Am J Anat 1971;132(2):179-88.

11. Majewska-Michalska E. Blood supply of the tegmentum mesencephali in dog. Folia Morphol (Warsz) 1984;43(1):35-41.

12. Majewska-Michalska E. Vascular architecture of the crura cerebri in dog. Folia Morphol (Warsz) 1986;45(2):151-7.

13. Majewska-Michalska E. Vascularization of the brain in guinea pig. II. Regions of vascular supply and spatial topography of the arteries in the particular parts of the brain. Folia Morphol (Warsz) 1995;54(1):33-40.

14. Majewska-Michalska E. Vascularization of the brain in guinea pig. IV. Angioarchitectonics of the tectum, tegmentum and crura mesencephali. Folia Morphol (Warsz) 1997;56(1):47-53.

15. Yoshida Y, Ikuta F. Three-dimensional architecture of cerebral microvessels with a scanning electron microscope: a cerebrovascular casting method for fetal and adult rats. J Cereb Blood Flow Metab[Online]1984; 4(2):290-6. Abstract from: NCBI Pubmed medline query: Unique Identifier 84212864.

16. Walker EP, Warnick F, Lange KV. Mammals of the world. Vol 1. Baltimore: Johns Hopkins; 1964.

17. Van Valen L. Tree shrews, primates and fossil. Evolution 1965;19:137-51.

18. Campbell CBG. Taxonomic status of tree shrews. Science 1966;22(734):436.

19. Lekagul B, McNeely A. A mammals of Thailand. Bangkok: Kurusapa Ladpraw; 1977.

20. Williams PL, Wawick R, Dyson M, Braunister LH. Gray's Anatomy. 37th ed. NewYork: Churchill Livingstone; 1989.

21. Geniec P, Korest DK. The neuronal architecture of the human posterior colliculus : A study with the Golgi method. Acta Oto-Laryngologica Suppl (Stockh) 1971;295:1-33.

22. Romanes GJ. Chuningham's manual of practical anatomy. Vol. III: Head and neck and Brain. 15th ed. New York: Oxford medical publications; 1993.

23. Kahle W, Leonhardt H, Platzes W. Color atlas and text of human anatomy .Vol. III: Nervous system and sensory organ. 4th revised ed. New York: Theime medical publishers; 1993.

24. Moore KL, Persaud TVN. The developing human: Clinically oriented embryology. 5th ed. Philadelphia: W.B. Saunders company; 1993.

25. Kaplan HA. Arteries of the brain: An anatomic study. Acta Radiol 1956;46:364-70.

26. Kaplan HA, Ford DH. The brain vascular system. Amsterdam: Elesevier; 1966.

27. Hassler O. Arterial pattern of human brainstem. Normal appearance and deformation in expanding supratentorial conditions. Neurology 1967;17(4):368-75.

28. Zeal AA, Rhoton AL. Microsurgical anatomy of the posterior cerebral artery. J Neurosurg 1979;48(4):534-59.

29. Marinković S, Millisavljević M, Kovačević M. Interpeduncular perforating branches of the posterior cerebral artery. Microsurgical anatomy of their extracerebral and intracerebral segments. Surg Neurol 1986; 26(4):349-59.

30. Saeki N, Rhoton AL. Microsurgical anatomy of the upper basilar artery and the posterior circle of Willis. J Neurosurg 1977;46(5):563-78.

31. Castaigne P, Lhermitte F, Buge A, Escourolle R, Hauw JJ, Lyon-Caen O. Paramedian thalamic and midbrain infarcts: Clinical and neuropathological study. Ann Neurol 1981;10(2):127-48.

32. Caruso G, Vincentelli F, Giudicelli G, Grisoli F, Xu T, Gouaze A. Perforating branches of the basilar bifurcation. J Neurosurg 1990;73(2):259-65.

33. Pedroza A, Dujovny M, Ausman JI, Diaz FG, Artero JC, Berman SK, et al. Microvascular anatomy of the interpeduncular fossa. J Neurosurg 1986;64(3):484-93.

34. Graff-Redford NR, Damasio H, Yamada T, Eslinger PJ, Damasio AR. Nonhaemorrhegical thalamic infarction: Clinical neuropsychological and electrophysiological findings in four anatomical groups defined by computerized tomography. Brain 1985;108(Pt 2):485-516.

35. Segarra JM. Cerebral vascular disease and behavior. I. The syndrome of the mesencephalic artery (basilar artery bifurcation). Arch Neurol 1970; 22(5):408-18.

36. Foix CH, Hillemand P. Les arters de láxe encéphalique jusqúau diencéphalon inclusivement. Rev Neurol (Paris) 1925a;32:705-39.

37. George AE, Raybaud CH, Salamon G, Kricheff I I. Anatomy of the thalamoperforating arteries with special emphasis on arteriography of the third ventricle: Part I. AJR 1975;124(2):220-30.

38. Marinković S, Gibo H. The surgical anatomy of the perforating branches of the basilar artery. Neurosurgery 1993;33(1):80-7.

39. Hochman MS, Sowers JJ, Bruce-Gregorios J. Syndrome of the mesencephalic artery: report of a case with CT and necropsy findings. J Neurol Neurosurg Psychiatry 1985;48(11):1179-81.

40. Tatemichi TK, Steinke W, Duncan C, Bello JA, Odel JG, Behrens MM, et al. Paramedian thalamopeduncular Infarction: clinical syndromes and magnetic resonance imaging. Ann Neurol 1992;32(2):162-71.

41. Pullicino P. Midbrain vascularity [Letter]. Neurology 1995;45(11):2122-3.

42. Milisavljević M, Marinković S, Malobabić S. Anatomic basis for surgical approach to the distal segment of posterior cerebral artery. Surg Radiol Anat 1988;10(4):159-66.

43. Mani RL, Newton TH, Glickman MG. The superior cerebellar artery: an anatomic roentgenographic correlation. Radiology 1968;91(6):1102-8.

44. Milisavljević M, Marinković S, Loić-Dragenić V, Djordjević L. Anastomoses in the territory of the posterior cerebral arteries. Acta Anat 1986;127 (3):221-5.

45. Lang J, Kapplinger E. A. laminae tecti (quadrigemina) and rami thalamogenicalati. Anat Anz [Online] 1980;147(1):1-11. Abstract from: NCBI Pubmed medline query: Unique Identifier 80240074.

46. Marinković S, Gibo H. The neurovascular relationships and the blood supply of the oculomotor nerve: the microsurgical anatomy of its cisternal segment. Surg Neorol 1994;42(6):505-16.

47. Gillilan LA. The correlation of the blood supply to the human brainstem with clinical brainstem lesions. J Neuropathol Exp Neurol 1964;23:78-108.

48. Ono M, Ono M, Rhoton AL, Barry M. Microsurgical anatomy of the region of the tentorial incisura. J Neurosurg 1984;60(2):365-99.

49. Marinković SV, Milisavljević MM, Kovačević MS. Anastomoses among thalamoperforating branches of the posterior cerebral artery. Arch Neurol 1986;43(8):811-4.

50. Holdorff H, Bradac GB. Intraparenchymatous pontomesencephalic vein: A radio-anatomical study. Acta Anat (Basel) 1974;89(3):333-44.

51.Tamaki N, Taomoto K, Fujiwara K, Matsumoto S, Takeda H. The venous drainage of the tectum mesencephali. An anatomical angiographic study of the quadrigeminal veins. Neuroradiology 1976;11(3):151-7.

52. Batson OV. Corrosion specimens prepared with a new materials. Anat Rec 1955; 121:425.

53. Murakami J. Application of the scanning electron microscope to the study of the find distribution of the blood vessels. Arch Histo Jap 1971;32:445-54.

54. Zimmer AE, Kim IH, Schlecter MM. Injection-corrosion casts of the central nervous system. J Neurosurg 1966;25(4):393-94.

55. Rodriguez-Baeza A, Reina-De La Torre F, Ortega- Sanchez M, Sahuguillo-Barris J. Perivascular structures in corrosion casts of the human central nervous system: a confocal laser and scanning electron microscope. Anat Rec 1998;252(2):174-84.

56. Reina-De La Torre F, Rodriguez-Baeza A, Sahuguillo- Barris J. Morphological characteristics and distribution pattern of the arterial vessels in human cerebral cortex: A scanning electron microscope study. Anat Rec 1998;251(1):87-96.

57. Anderson WD, Anderson BG, Sagnin RJ. Arterial supply and venous drainage of the brain of black bear (*Ursus americanus*) I. Gross anatomical distribution. Acta Anat 1989;135(1):281-4.

58. Anderson WD, Anderson BG, Sagnin RJ. Arterial supply and venous drainage of the brain of black bear (*Ursus americanus*) II. Intracranial microvasculature. Acta Anat 1989;135(1):285-8.

59. Ritonga M. Vascularization of common tree shrew' s olfactory bulb as revealed by plastic corrosion cast technique and view under SEM. [M.S. Thesis in Anatomy]. Bangkok: Faculty of Graduate Studies, Mahidol University; 1989.

60. Sudwan P, Chunhabundit P, Bamroongwong S, Rattanachaikunsopon P, Somana R. Hypophyseal angioarchitecture of common tree shrew (*Tupaia glis*) revealed by scanning electron microscopy of vascular corrosion casts. Am J Anat 1991;192(3):263-73.

61. Chunhabundit P, Somana R. Scanning electron microscopic study on pineal vascularization of the common tree shrew (*Tupaia glis*). J Pineal Res 1991;10(2):59-64.

62. Poonkhum R, Pongmayteekul S, Meeratana W, Pradidarcheep W, Tongpila S, Mingsakul T, et al. Cerebral microvascular architecture in the common tree shrew (*Tupaia glis*) revealed by plastic corrosion casts. Microscopy Research and Technique 2000 (Inpress).

63. Kompatraporn N. Cerebellar microvascularization in common tree shrew (*Tupaia glis*). [M.S. Thesis in Anatomy]. Bangkok: Faculty of Graduate Studies, Mahidol University; 1998.

64. Kimmaktong W. Hypothalamic vascularization in common tree shrew (*Tupaia glis*) as revealed by vascular corrosion cast/ SEM technique. [M.S. Thesis in Anatomy]. Bangkok: Faculty of Graduate Studies, Mahidol University; 1998.

65. Mingsakul T. Ultrastructure and microangioarchitecture of the choroid plexus in the common tree shrew (*Tupaia glis*). [Ph.D. Thesis in Anatomy]. Bangkok: Faculty of Graduate Studies, Mahidol University; 1998.

66. Lametschwandtner A, Albrecht U, Adam H. The vascularization of the anuran brain. The mesencephalon. A SEM study of vascular corrosion casts. Acta Zool (Stockh) 1978;60:89-92.

67. Laemle LK. Retinal projections of *Tupaia glis*. Brain Behav Evol 1968;1(5):473-99.

68. Campbell CBG. The retinal projection of the tree shrew and hedgehog. Brain Res 1967;5(3):406-18.

69. Chunhabundit P, Somana R. Modification of plastic mixture for vascular corrosion cast to withstand electron beam at high magnification under SEM. Proc 4th Asia-Pacific Conference and Workshop on Electron Microscope. Bangkok, Thailand, 1988:411-412.

70. Bamroongwong S, Somana R, Chunhabundit P, Rattanachaikunsopon P. Scanning electron microscopic study of the splenic vascular casts in common tree shrew (*Tupaia glis*). Anat Embryo 1991;184(3):301-4.

71. Campbell CBG. The relationships of the tree shrews: The evidence of the nervous system. Evolution 1966;20:276-81.

72. Crosby EC, Woodburne RT. The mammalian midbrain and isthmus region: The nuclear pattern of the non-tectal portions of the midbrain and isthmus in primates. J Comp Neurol 1943c;78:441-82.

73. Harting JK, Hall WC, Diamond IT, Martin GF. Anterograde degeneration study of the superior colliculus in *Tupaia glis*: evidence for a subdivision between superficial and deep layers. J Comp Neurol 1973b;148(3):361-86.

74. Casagrande VA, Harting JK, Hall WC, Damond IT, Martin GF. Superior colliculus of the tree shrew (*Tupaia glis*): evidence for a structural and functional subdivision into superficial and deep layers. Science 1972; 177(47):444-7.

75. Casagrande VA, Diamond IT. Ablation study of the superior colliculus in the tree shrew (*Tupaia glis*). J Comp Neurol 1974;156(2):207-38.

76. Cassaday JH, Jones DR, Diamond IT. Projections from cortex to the tectum in the tree shrew, *Tupaia glis*. J Comp Neurol 1979;185(2):253-92.

77. Albano JE, Humphrey AL, Norton TT. Laminar organization of the receptive-field properties in tree shrew superior colliculus. J Neurophysiol 1978;41(5): 1140-54.

78. Albano JE, Norton TT, Hall WC. Laminar origin of the projections from the superficial layers of the superior colliculus in the tree shrew, *Tupaia glis*. Brain Res 1979;173(1):1-11.

79. Gordon B. Receptive fields in deep layers of cat superior colliculus. J Neurophysiol 1973, 36(2):157-78.

80. Huber GC, Crosby EC. The comparison of the mammalian and reptilian tecta. J Comp Neurol 1943;78:133-68.

81. Robson JA, Hall WC. Projection from the superior colliculus to the dorsal lateral geniculate nucleus of the gray squirrel (*Sciurus carolinensis*). Brain Res 1967;113(2):379-85.

82. Altman J, Bayer SA. Time of origin of neurons of the rat superior colliculus in relation to other components of the visual and visuomotor pathways. Exp Brain Res 1981;42(3-4):424-34.

83. Kawamura S, Sprague JM, Niimi K. Corticofugal projections from the visual cortices to the thalamus, pretectal and superior colliculus in the cat. J Comp Neurol 1974;158(3):339-62.

84. Cassaday JH, Diamond IT, Harting JK. Auditory pathways to the cortex in the *Tupaia glis*. J Comp Neurol 1976;166(3):303-40.

85. Morest DK, Oliver DL. The neuronal architecture of the inferior colliculus in the cat: defining the functional anatomy of the auditory midbrain. J Comp Neurol 1984;222(2):209-36.

86. Carpenter MB. A study of the red nucleus in rhesus monkey. J Comp Neurol 1956;105(2):195-250.

87. Otabe JS, Horowitz A. Morphology and cytoarchitecture of the red nucleus of the domestic pig (*Sus scrofa*). J Comp Neurol 1970;138(3):373-90.

88. Gillilan LA. The mammalian midbrain and isthmus region: The nuclear pattern of the non-tectal portions of the midbrain and isthmus in rodents. J Comp Neurol 1943a;78:213-51.

89. Crosby EC, Woodburn RT. The mammalian midbrain and isthmus region: The nuclear pattern of the non-tectal portions of the midbrain and isthmus in the shrew and the bat. J Comp Neurol 1943b;78:253-88.

90. Brown JO. The mammalian midbrain and isthmus region: The nuclear pattern of the non-tectal portions of the midbrain and isthmus in the dog and cat. J Comp Neurol 1943;78:365-405.

91. Crosby EC, Woodburn RT. The mammalian midbrain and isthmus region: The nuclear pattern of the non-tectal portions of the midbrain and isthmus in the armadillo. J Comp Neurol 1943a;78:191-211.

92. Gillilan LA. The mammalian midbrain and isthmus region: The nuclear pattern of the non-tectal portions of the midbrain and isthmus in ungulates. J Comp Neurol 1943b;78:289-364.

93. Tamthai B. The mammalian midbrain and isthmus region: The nuclear pattern of the non-tectal portions of the midbrain and isthmus in the mink. J Comp Neurol 1943;78:407-40.

94. Woodburn RT.The mammalian midbrain and isthmus region: The nuclear pattern of the non-tectal portions of the midbrain and isthmus in the opossum. J Comp Neurol 1943;78:169-90.

95. Hanaway J, McConnell JA, Netsky MG. Cytoarchitecture of the substantia nigra in the rat. AM J Anat 1970;129(4):417-38.

96. Ma TP, Hazlett JC. Cytoarchitecture of the substantia nigra pars lateralis in the opossum (*Didelphis virginiana*): A correlated light and electron microscopic study. Anat Rec 1995;241(4):564-78.

97. Marsden CD. Pigmentation in the nuclear substaniae nigrae of mammals. J Anat 1961;95(2):256-61.

98. Lee RM. Morphology of cerebral arteries. Pharmacol Ther 1995,66(1):149-73.

99. Alpers BJ, Berry GR, Paddison RM. Anatomical studies of the circle of Willis in normal brain. Arch Neurol Psychiat 1959;81:409-18.

100. Lake AR, Van Niekerk IJM, Le Roux CGJ, Trevor-Jones TR, Dewet PD. Angiology of the brain of the baboon *Papio ursinus*, the vervet monkey *Cercopithecus py gerithrus*, and the bush baby *Galago senegalensis*. Am J Anat 1990;187(3):277-87.

101. Pedroza A, Dujovny M, Artero JC, Umansky F, Berman SK, Diaz FG, et al. Microanatomy of the posterior communicating artery. Neurosurgery 1987;20(2):228-235.

102. Shontz C, Dujovny M, Ausman JI, Diaz FG, Pearce JE, Berman SK, et al. Surgical anatomy of the arteries of the posterior fossa. J Neurosurg 1986;64(4): 540-4.

103. Kaplan H, Rabiner AM, Browder J. Anatomical study of the arteries of the midbrain, pons and medulla. Trans Am Neurol Assoc 1953;78:54-6.

104. Willams DJ. Origin of the posterior cerebral artery. Brain 1936;509:175-80.

105. Percheron G. Arteries of the human thalamus. II. Arteries and paramedian thalamic territory of the communicating basilar artery. Rev Neurol (Paris) 1976;132(5):309-24.

106. Waterston JA, Stark RJ, Gilligan BS. Paramedian thalamic and midbrain infarction: The 'mesencephalothalamic syndrome'. Clin Exp Neurol 1987 ;24:45-53.

107. Savoirdo M, Girotti F. Micrographia after thalamo-mesencephalic infarction. Neurology. 1999;52(9):1921-2.

108. LeWitt PA. Micrographia after thalamo-mesencephalic infarction. Neurology. 1999;52(9):1921-2.

109. Tatu L, Monlin T, Bogousslavsky J, Duvernoy H. Arterial territories of human brain: brainstem and cerebellum. Neurology 1996;47(5):1125-1135.

110. Hara K, Fujino Y. The thalamoperforatic artery. Acta Radiol (Diagn) 1966;5:192- 200.

111. Boiaekina IV. Neurono-vascular relations in the superior colliculus of the cat tectum mesencephali. Arkh Anat Gistol Embriol [Online] 1982;83(9):34-

7. Abstract from: NCBI Pubmed medline query: Unique Identifier 83099885.

112. Graham J, Casagrande VA. A light microscopic and electron microscopic study of the superficial layers of the superior colliculus of the tree shrew (*Tupaia glis*). J Comp Neurol 1980;191(1):133-51.

113. Nakahara T, Oki S, Multaqin Z, Tokuda Y, Emoto K, Kuwabara S, et al. An investigation of the vascular anatomy and microvascular architecture of the brainstem in cats. Hiroshima J Med Sci 1990;39(3):83-8.

114. Banafe A, Manelfe C, Scotto B, Pradere MY, Rascol A. Role of computed tomography in vertebrobasilar ischemia. Neuroradiology 1985;27(6):484-93.

115. Chuncher S. Microvascularization of thalamus and metathalamus in common tree shrew (*Tupaia glis*). [M.Sc. Thesis in Anatomy]. Bangkok: Faculty of Graduate Studies, Mahidol University; 1999.

116. Wislocki GB. The unusual mode of development of the blood vessels of opossum's brain. Anat Rec 1939;74:409-27.

117. Bertossi M, Mancini L, Favia A, Nico B, Ribotti D, Virgintino D, et al. Permeability-related structures in developing and mature microvessels of the chicken optic tectum. Biol Struct Morphog 1992;4(4):144-52.

118. Issidorides MR. Neuronal vascular relationships in the zona compacta of the normal and parkinsonian substantia nigra. Brain Res 1971;25(2):289-99.

119. Finley KH. Angio- architecture of the substantia nigra and its pathogenic significance. Arch Neurol Psychiat 1936;36:118-27.

120. Hough HB, Wolff HG. The relative vascularity of subcortical ganglia of the cat's brain; The putamen, globus pallidus, substantia nigra, red nucleus, and geniculate bodies. J Comp Neurol 1939;71(3):427-36.

121. Felten DL, Crutcher KA. Neuronal-vascular relationships in the raphe nuclei, locus coeruleus, and substantia nigra in primates. J Anat 1979; 155(4) :467-82.

122. Creaigie EH. On the relative vascularity of various parts of the central nervous system of the albino rat. J Comp Neurol 1920;31:429-64.

123. Andrew DLE, Patterson JA. Postnatal development of vascularity in the inferior colliculus of the young rat. Am J Anat 1989;186(4):389-96.

124. Gross PM, Sposito NM, Petterson SE, Panton DG, Fenstermacher DJ. Topography of capillary density, glucose metabolism and microvascular function within the rat inferior colliculus. J Cereb Blood Flow Metab 1987;7(2):154-60.

125. Hassler O. Deep cerebral venous system in man: a microangiographic study on its areas of drainage and its anastomoses within the superficial cerebral veins. Neurology 1966;16(5):505-11.

126. Ono M, Rhoton AL, Peace D, Rodriguez RJ. Microsurgical anatomy of the deep venous system of the brain. Neurosurgery 1984;15(5):621-57.

127. Matsushima T, Rhoton AL, De Oliveira E, Peace D. Microsurgical anatomy of the veins of the posterior fossa. J Neurosurg 1983;59(1):63-105.

128. Andeweg J. Consequences of the anatomy of deep venous outflow from the brain. Neuroradiology 1999;41(4):233-41.

129. Amstrong LD, Horowitz A. The brain venous system of the dog. Am J Anat 1971;132(4):479-90.

130. Huang YP, Wolf BS. The veins of the posterior fossa-Superior or galenic draining group. AJR 1965;95(4):808-21.

131. Huang YP, Wolf BS, Antin SP. The veins of the posterior fossa-Anterior or petrosal draining group. AJR 1968;104(1):36-56.

132. Wolf BS, Huang YP, Newman CM. The lateral anastomotic mesencephalic vein and other variations in drainage of the basal cerebral vein. AJR 1963; 89(2):411-22.

133. Gregory WK. The orders of mammals, Part. 2: Genetic relations of the mammalian orders. Bull Amer Mus Nat Hist 1910;27:105-524.

134. Le Gros Clark WE. The thalamus of *Tupaia minor*. J Anat (Lond) 1929;63:177-206.

135. Simpson GG. The principles of classification and a classification of mammals. Bull Amer Mus Nat Hist 1945;84:1-350.

136. Nepier J, Nepier PH. A handbook of living primates. New York: Academic Press; 1967.

137. Martin RD. Primate origins and evolutions: a phylogenetic reconstruction. London: Chapman and Hall; 1990.

138. Campbell CBG. The relationships of the tree shrews: the evidence of the nervous system. Evolution 1966;20:276-281

139. Schneider GE. Two visual system: brain mechanisms for localization and discrimination are dissociated by tectal and cortical lesions. Science 1969;163(870):895-902.

140. Corbet GB, Hill JE. World list of mammalian species. 3rd. London: Natural History Museum; 1991.

APPENDIX I

The common Tree Shrew

Taxonomic Status

Kingdom: Animal

Subkingdom: Metazoa

Branch: Enterozoa

Division: Bilateria

Section: Eucoelomata

Phylum: Chordata

Group: Craniata

Subphylum: Gnathostomata (Jawed Vertebrates)

Superclass: Tetrapoda

Class: Mammalia

Subclass: Eutheria

Order: Primate or Insectivore or Scandentia

Suborder: 1. Prosimii

Infraorder: Lamuriformes

2. Menotyphla

Family: Tupaiidae

Subfamily: Tupaiinae

Genus: Tupaia

Species: glis

Subspecies: At least 13 subspecies

Synonyms

Serex glis (Diard, 1820)

Tupaia feruginea (Raffles,1821)

Tupaia müllendorffi (Matschie, 1898)

Tupaia sordida (Miller, 1900)

Tupaia chrysomalla (Miller,1900)

Tupaia phaeura (Miller,1902)

Tupaia castanea (Miller,1903)

Tupaia pulonis (Miller,1903)

Tupaia tephrura (Miller,1903)

Tupaia chrysogastra (Miller,1903)

Tupaia discolor (Lyon, 1906)

Tupaia siaca (Lyon, 1908)

Tupaia lacernata (Thomas& Wroughton, 1909)

Tupaia cuyonis ((Miller,1910)

Tupaia raviana (Lyon, 1911)

Tupaia pemangilis (Lyon, 1911)

Tupaia obscura (Kloss, 1911)

Tupaia riabus (Lyon, 1913)

Tupaia anabae (Lyon, 1913)

Vernacular Names

Common tree Shrew

Spitzhörnchen

Tupaia furrugineux

Painted tree shrew

Mill's tree shrew

Tupajas

Topaies

Tupayes

Tupaide's

Diagnosis

A large tree shrew with a bushy tail that is slightly less to a little more than body length.

Distribution

From Nepal and Sikkim east South China and throughout Southeast Asia to Indonesia but not in Philippine. In Thailand, the following are Thai subspecies that divided into mainland and island subspecies.

Mainland subspecies:

1. *Tupaia glis ferruginea*
2. *Tupaia glischinensia*
3. *Tupaia gliswilkensoni*

4. *Tupaia glis charissa*
5. *Tupaia glis belangeri*
6. *Tupaia glis laotum*
7. *Tupaia glis olivacea*
8. *Tupaia glis concolor*

Island subspecies:

1. *Tupaia glis larcernata*
2. *Tupaia glis cognata*
3. *Tupaia glisoperosa*
4. *Tupaia glis ultima*
5. *Tupaia glis sinus*

Characteristics of common tree shrew

Morphological characteristics

Size	Male	Female
Body length (mm):	161-240	175-240
Tail length (mm):	145-196	140-190
Weight average (g):	177	159

Color: The dorsal parts are red-dish, olive, shades of brown and gray to almost black

: The ventral part is whitish or buff to dark brown

Cranium: Primate-like, rounder, elongated muzzle and small brain case laterally directed orbits but show a part orbital bar

Brain: More complex than that insectivore, the olfactory center reduced, the visual apparatus enhanced, neocortex expanded

Nose: Elongated shrew-like nose terminating in a naked moist snout

Long whiskers: Absent

Eyes: Relatively large, located in the anterolateral side of head and completely encircled by bone

Ears: Quite human inform

Dental formula: Total teeth are 38

Incisor	Canine	Premolar	Molar
$\frac{2}{3}$	$\frac{1}{1}$	$\frac{3}{3}$	$\frac{3}{3}$

Limbs:

Forelimb: Highly mobility, bones of the forearm articulate to allow pronation and supination. Thumb can oppose to the other digits but limited extent

Hindlimb: Longer than forelimb, tibia and fibula are joined by ligaments that can not rotate. Ankle joint can perform lateral movement

Digits: Five fully formed digits on each hand and foot, all digits bear claws, not nails and fully opposable

Tail: Long and slender, but well haired, the longer hairs are confined to the dorsal surface but the ventral surface lacking long hairs

Chromosome: Diploid number =60

Reproductive system:

In female: Mammae: 1-3 pairs, Uterus: Bicornuate

In male: Testis: Scrotal testes, Penis: Pendulous penis

***Tupaia glis* is distinguished from other general of tree shrew by this feature:**

1. The lower lobe of the ear is smaller than the upper part.
2. The naked area on top of the nose is cut squarely across instead of being slightly prolonged backward in the midline.
3. The tail is covered by long hairs.

The main similarities between tree shrew and primates:

Skull: Snout relatively short, enlarged, forward-facing orbits, postorbital bar present, pattern of bones in medial orbital wall, enlarged braincase, advanced form of auditory ossicles

Dentition: Tooth comb present in front of lower jaw

Limbs: Highly mobile, ridged skin on palms and soles, five fully formed digits on each hand and foot, grasping hand characteristic

Brain and sense organ: Olfactory apparatus reduced, visual apparatus enhanced, avascular area of macula, neocortex expanded, calcarine sulcus present

Reproductive: Pendulous penis, scrotal testes, discoidal placenta and small number of feat

Miscellaneous: Caecum present

The main similarities between tree shrews and insectivore:

1. All digits bear claws and not nails
2. The vision is not fully stereoscopic
3. The auditory bulla is constituted from the entotympanic bones and not the petrosal or petrosal plus the ectotympanic

Ecology and Behavior

The common tree shrews actually spend much of their time on the ground foraging on the forest floor and generally omnivorous, eating anything they come across, including ants, termites, beetles, fruit, spiders, seeds, bugs and even lizards and small rodents. There is no evidence that they shovel through the forest litter as shrews do.

Tree shrews are nervous and aggressive animals. Males will not tolerate the presence of other males, through there seems to be little fighting between the sexes. They typically form pairs which are strongly territorial and follow the same pathways within their territory. They are very fond of water and often bath in water-filled hollows of tree.

There is no indication of a breeding season. Pregnancies have been observed to be associated with the period of low rainfall; June, July and August. Nests are built in hole in fallen trees, hallow bamboo or similar site. The gestation period is approximately 41-50 days. The numbers of young are 1-4 (usually 2). Newborn is pink, hairless and has closed eyes. Pigmentation appears on the fourth day. Hair begins to grow on the fifth day. Teeth begin to appear about the eleventh day and the

eyes open on the twenty-fifth day. At sixth months, they are sexually mature. Longevity is 2-3 years, with the maximum of 5.5 years in captivity.

APPENDIX II

Batson's # 17 Plastic Mixture for Vascular Casting

Plastic Mixture Preparation

Batson's # 17 Monomer base solution*	12.5 ml
Batson's # 17 Catalyst*	3.5 ml
Batson's # 17 Promoter*	0.5 ml
Acron Denture Base **	6.5 ml

Prepared in an ice bath, the solution are mixed thoroughly and used immediately.

* Batson's corrosion kit can be obtained from:

Polyscience, Inc.

Paul Valley Industrial Park

Warring, Pa. 18976 USA

** Acron Denture Base can be obtained from:

Yoawarach

Bangkok, Thailand

APPENDIX III

Bouin's Solution (Bouin, 1897)

Saturated aqueous picric acid	750 ml
40% Formaldehyde	250 ml
Glacial acetic acid	50 ml

Bouin's solution is not used in histochemistry but preserves morphological features, especially of connective tissue. This fixative is valuable for purely histological work because physical distortion of tissue is minimal. However, intracellular structures other than nuclei are poorly preserved. Specimens are usually fixed in Bouin's solution for 24 hours, but material stored in it for several months is sometimes still usable. Each of Bouin's solution composition is described following:

1. Picric acid [$C_6H_2(NO_2)_3OH$ or 2,4,6- trinitrophenol]

Picric acid is trinitrophenol. It is a much stronger acid than unsubstitited phenol aqueous solution owing to the electron-withdrawing effect of the three-nitro groups on the hydroxyl group:

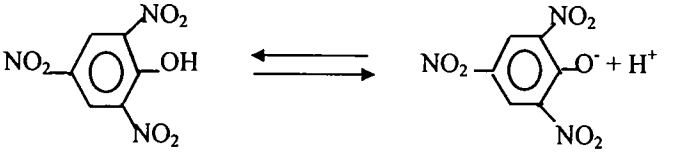

Trinitrophenol is a bright yellow solid. It is dangerously explosive when dry and is therefore stored under water. It is sparingly soluble in water (about 1% at room temperature) but more so in alcohol (nearly 5%) and benzene (10%).

2.Formaldehyde

formaldehyde is a gas (-21°C) with the structural formula 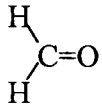

It is solution in water to containing 37-40% by weight of the gas in water and sold under the name of 40% formaldehyde or formalin. In aqueous solution, formaldehyde is present as methylene hydrate or methylene glycol, the product of the reaction:

$$H_2C{=}O + H_2O \rightleftharpoons HOCH_2OH$$

Therefore, formalin also contains solution polymers of the form HO(CH2O)nH (n = 2-8), know as lower polyoxymethylene glycol. The polymers are hydrolyzed when formalin is diluted with on excess of water. Thus, trioxymethylene glycol ($HO(CH_2O)_3H$): $HO(CH_2O)_3H + 2H_2O \rightleftharpoons 3HOCH_2OH$. Formalin also contains methanol (commonly about 10% v/v) which is added a stabilizer to inhibit the polymerization. Methanol is formed by formaldehyde a hemiacetal (methylal), Which is more stable than methylene hydrate:

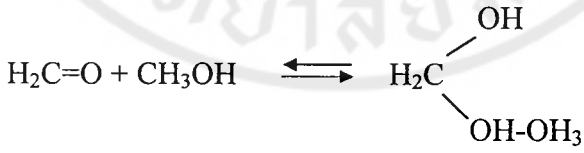

The content of formaldehyde in a fixative is best denoted by stating the percentage by weight of the gas rather than the amount of formalin used in preparing the mixture. Thus, 4% formaldehyde is referred to 10% formalin (for the same solution), though the latter designation is in common use.

Formaldehyde reacts with several parts of protein molecules. The methylene glycol molecule added to many functional groups to form hemiacetal and related adducts. For example, with primary amines (N-terminal amino acids and lysine side-chain):

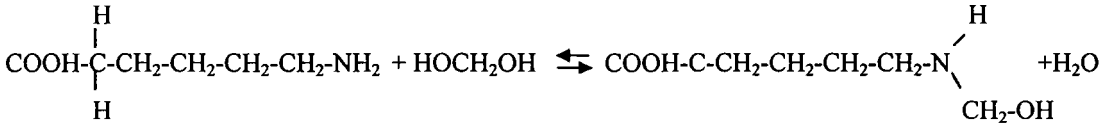

This reaction are all readily reversible by washing in water or alcohol. However, the hemiacetal-like adducts all have free hydroxymethyl groups and there are capable of further reaction with functional groups of protein:

Thus, different protein molecules can be joined together by methylene bridges, which are chemically stable. Cross-linking of protein molecules by formaldehyde is much slower than the other fixative agents and requires 1-2 weeks for completion at room temperature. For non-histological methods especially for the nervous system, work better after complete fixation very long periods of storage in the formaldehyde solution results in excessive hardening, loss stain ability of nuclei.

Formaldehyde preserves most lipids. The chemical reactions of formaldehyde with lipid under ordinary conditions of fixation are 1). Addition to the amine groups of phosphatidyl ethanolamine which is probably reversible by washing in water 2). Prevention of the histochemical reactivity of plasmologens owing to oxidation, probably to a glycol, of the ethylenic linkage next to the other group.

Formaldehyde dose not react with carbohydrate. All common mucosubstances can be demonstrated after fixation with formaldehyde through appreciable quantities of glycogen are lost. Bouin's solution are preferable to formaldehyde because 1). It protects the tissue against damaging effects of embedding in wax, and 2). Staining with almost of dyes is brighter then after formaldehyde alone. In addition, formalin gives off an unpleasant vapor that causes irritable to the eyes, respiratory epithelium and unpleasant "formalin dermatitis" after immersion of hands in this solution.

3.Glacial acetic acid (CH_3COOH)

Pure acetic acid is called "glacial" because it solidifies at 17°C if water free. It does not fix protein, but it coagulates nucleic acids. The mechanism by which this change is brought about is obscure. Gracial acetic acid is included in fixative mixtures to preserve chromosomes, precipitate the chromatin of interphase nuclei and oppose the shirking actions of other agents such as ethanol and picric acid.

APPENDIX IV

Cresyl Fast Violet Stain Paraffin Section

Fixative: Bouin's solution

Section: Paraffin section at 10 μm

Preparation of stain:

Cresyl Fast Violet (Cresyl Violet Acetate)	1 g
Distilled Water	100 ml

Method:

1. Dewax section and remove wax with xylene, rinse in second dish of xylene.
2. Rinse in absolute, 95%, 90%, 80%, 70% alcohol and bring to distilled water.
3. Cover with filtered cresyl fast violet, stain for 20-30 minutes.
4. Wash in distilled water and place in 70%, 80%, 90% alcohol.
5. Leave in 95% alcohol until excess stain has been removed.
6. Pass through absolute alcohol into three changes of xylene and mount in Canada balsam.

Results:

- Nissl substance — deep purple-dark blue
- Nuclei and some cytoplasmic process of neuron — purple-blue
- Background — colorless

Note:

1. Cresyl Violet Acetate (No C.I. number; M.W. 321)

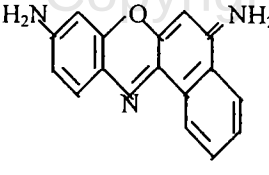

Cresyl Violet Acetate is the modern equivalent of cresyl fast violet (cresyl echt violet). Both are often loosely formed "cresyl violet". They are useful as violet cationic dyes, soluble in water and alcohol. They are popular as "Nissl stains" for nervous tissue. Basing on the structures of the major chromopholic systems, cresyl violet acetate is synthetic oxazine dye which consists of the oxazine chromophore [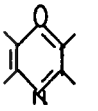]. The oxazine chromophore has obvious similarity to those of the azine and thaizine dyes and exists in o-quinonoid form (with positive change attributed to the oxygen) and p-quinonoid form.

2. If only Nissl substance in required to be demonstrated the stain is acidified with 0.25 percentage acid.

APPENDIX V

Film Processing for SEM Photograph

Negative Film Processing

1. Load the exposed film into the film holder in the dark room.
2. Wash the film in the cool distilled water (20-21°C) for 1 minute to clear the excessive softening of the emulsion.
3. Develop with Microdol-X (22°C) with continuously stirred for 12.5 minutes to silver metallic under alkaline condition.
4. Wash in the distilled water for 1 minute.
5. Place in stop bath (acetic acid) for 1 minute to stop the reaction of the developer.
6. After washing in the distilled water for 1 minute, the film is immersed in a fixer to convert silver thiosulfate that is water-soluble. this step is under acidic condition which will neutralize excess alkaline developer that preventing film fog.
7. Wash in distilled water before placing in hypoclearing agent for 2 minutes.
8. The well developed film can be visualized under the room light. It is rinsed in the tap water for 10-15 minutes before dipping in the water-repellent fluid (photo flo) for 1-2 minutes to prevent water spots.
9. Finally, the film is dried in the film dryer or left in the opened air.

Note:

1. The process of film development involves a redox reaction. Black and white photographic film contains small grains of silver bromide, evenly over a thin gelatin coating on paper. Exposures of the film to light activates silver bromide as follow:

$$AgBr + Light \longrightarrow AgBr^{*} \text{ (AgBr affected by light)}$$

Next, the exposed film is treated with a developer, a solution containing a mild reducing agent such as hydroquinone as follows:

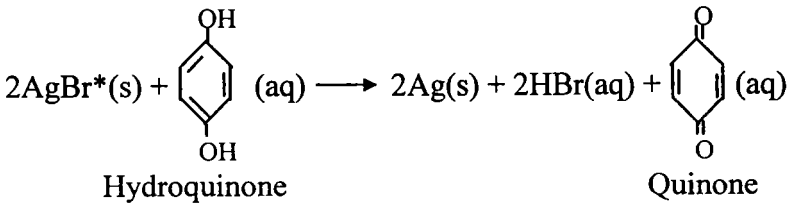

Hydroquinone Quinone

In this redox process, The Ag^+ ions in the activated AgBr are preferentially reduced to metallic (silver) while hydroquinone is oxidized to quinone. After placing in acetic acid ($HC_2H_3O_2$) to complete reaction with hydroquinone, the unreacted AgBr must be removed from the film by treated with a fixer. The fixer is a solution containing sodium thiosulfate ($Na_2S_2O_3$) to removed the silver ions:

$$AgBr(s) + 2S_2O_3^{2-}(aq) \longrightarrow Ag(S_2O_3)_2^{3-}(aq) + Br^-(aq)$$

Enlargement and Printing

The quality of the negative film should be evaluated prior enlarging. To classified the quality according to the contrast are three groups. The low contrast negative film requires high contrast papers (BH papers), while the medium to high contrast negative film should require the normal to low contrast papers (BN to BS papers). The process of enlargement and printing is done under the safe light as follows:

1. Place the negative film on the negative holder by emulsion down.
2. Turn on the light source of enlarger and open the aperture widely.
3. Adjust the enlarger by either raising up or lowing down for the appropriated size as need. The image is projected on the easel.
4. The sharp grains on the image, seeing with the image focuser, is adjusted by focusing knob.

5. Adjust the easel until the image fills on the paper.
6. Set the appropriate aperture.
7. Turn off the light of the enlarger and set the proper exposure time.
8. Place the photographic paper in the easel, turn on the light of the enlarger and allow exposing it for the desired time.
9. Take the exposed paper and submerged in developer (Dextol:water = 1:2).
10. Transfer the developed paper to stop bath for 20 to 30 second minutes.
11. Rinse in running tap water and dip in fixer for fixer for 15 minutes.
12. Wash the photograph in running tap water for 30 minutes to 1 hour.
13. Submerge in a dilute water-repellent agent (Photo flo) for 15 minutes.
14. Dry with the print dryer or air dry and the scanning electron micrograph is now ready for evaluation.

BIOGRAPHY

NAME Miss Churairat Duangchan

DATE OF BIRTH 28 July 1970

PLACE OF BIRTH Petchaburi, Thailand

INSTITUTIONS ATTENDED Prachomklao Nursing College, Petchaburi,1989-1993: Diploma in Nursing (Equivalent to Bachelor of Science in Nursing) Mahidol University, 1998-2000: Master of Science (Anatomy)

POSITION & OFFICE 1993-Present, Prachomklao Nursing college, Petchaburi, Thailand. Position : Instructor